NASTRAN ANALYSIS OF THE 1/8-SCALE SPACE SHUTTLE DYNAMIC MODEL

By Murray Bernstein, Philip W. Mason, Joseph Zalesak,
David J. Gregory, and Alvin Levy

Grumman Aerospace Corporation

INTRODUCTION

The Space Shuttle configuration has more complex structural dynamic characteristics than previous launch vehicles primarily because of the high modal density at low frequencies and the high degree of coupling between the lateral and longitudinal motions. An accurate analytical representation of these characteristics is a primary means for treating structural dynamics problems during the design phase of the Shuttle program. The 1/8-scale model program was developed to explore the adequacy of available analytical modeling technology and to provide the means for investigating problems which are more readily treated experimentally. The basic objectives of the 1/8-scale model program are

(1) To provide early verification of analytical modeling procedures on a Shuttle-like structure

(2) To demonstrate important vehicle dynamic characteristics of a typical Shuttle design

(3) To disclose any previously unanticipated structural dynamic characteristics

(4) To provide for development and demonstration of cost effective prototype testing procedures

This paper constitutes a progress report on the program to date.

The work described herein has been conducted primarily under contract for the NASA Langley Research Center.

DESCRIPTION OF STRUCTURAL MODEL

The model is designed to represent the important structural dynamics characteristics of a Shuttle-like vehicle while keeping the fabrication costs low.

The general arrangement of the model is shown in figure 1. The original basis for the design was a 21.35 MN (4.8×10^6 lb) GLOW, 55.474 m (182 ft) long parallel burn configuration (Grumman Design 619). Subsequently, under Rockwell International sponsorship, the forward solid rocket booster to external tank attachment design was modified to a single point connection representing the RIC prototype as of December 1972.

Figure 1 illustrates a mock-up of the 1/8-scale model which is approximately 7.315 m (24 ft) from the external tank nose cone to the solid rocket booster tie-down plane. The total model is composed of 4 major comporents: the Orbiter, external tank, and two solid rocket boosters. The Orbiter is shown in figure 2, without the cargo bay doors, and in figure 3 with the cargo bay doors and nonstructural plastic fairings that complete the contours of the vehicle.

Figure 4 shows the Orbiter fuselage under assembly and figure 5 is a NASTRAN plot of the finite-element model. The fuselage structural model is approximately 3.543 m (11.625 ft) long, contains 21 frame stations, and is constructed of 2024 aluminum. The bottom shell of the fuselage is 0.635 mm (0.025 in.) thick while the side walls and top shell are 0.508 mm (0.020 in.) thick. The cargo bay doors are made up of segments of 0.4064 mm (0.016 in.) aluminum sheet that are attached to the frames. The details of the attachment to the frames prevent the doors from resisting fuselage bending but allow them to act in resisting shear.

The fuselage frames in the region of the cargo bay are constructed of aluminum sheet that has been bent to form a channel section. The tapered side wall channel section and the lower portion are attached back to back to form a U-shaped frame. The major bulkheads are of stiffened sheet construction.

The delta wing shown in figure 6 consists of 6 spars and 4 ribs that are formed from 0.8128 mm (0.032 in.) 2024 aluminum sheet. The covers are 0.5080 mm (0.020 in.) thick. NASTRAN plots of the finite-element model are shown in figures 7 and 8.

The fin structure, which includes only the structure from the fuselage to the center of gravity of the physical fin model, contains 3 spars and a closure rib. The webs are 0.8128 mm (0.032 in.) thick while the covers are 0.5080 mm (0.020 in.) thick. NASTRAN plots of the finite-element model are shown in figures 9 and 10.

A NASTRAN plot of the cargo bay doors is shown in figure 11 and a schematic illustrating the connection of the door shell to the door frames is shown in figure 12.

The external tank contains four main components, the LOX tank, inter tank skirt, LH_2 tank, and the aft tank skirt. A NASTRAN plot of the entire structure is shown in figure 13. The total structure is approximately 6.858 m (270 in.) long and has a radius of 0.5029 m (19.8 in.). The orbiter interstage points are located totally within the LH_2 part of the external tank; the forward interstage at station 148.756 transmits vertical and side loads while the aft center-line interstage at station 245.7536 transmits thrust and side load. Inclined bars also at station 245.7536 connect with the orbiter at B.L. 13.75 and with the tank at B.L. 16.4631 to provide the necessary determinate supports. The solid rocket booster is connected to the tank at the forward end at the inter tank skirt. This pin connection transfers vertical, side, and all drag loads. The aft tank/SRB interstage is located at tank station 270.988 and consists of 3 bars capable of transmitting vertical and side load as well as roll moment.

The liquid oxygen tank, figure 14, is a shell of revolution composed of a conical shell, a cylindrical shell, and two quasi elliptical end domes which are each formed from two tangential spherical segments. The overall length is 1.98 m (78 in.). The tank is 2219 aluminum and all shell segments are welded at the joints. The primary gage is 0.508 mm (0.020 in.) with the lower dome being 0.406 mm (0.016 in.), and the total tank structure is connected to the inter tank skirt via a Y-ring located at the aft end of the cylindrical portion of the tank.

Figure 15 shows the liquid oxygen tank connected to the inter tank skirt and to the forward tank/SRB interstage. Figures 16, 17, and 18 show additional details of the external tank structure. The LOX tank is of monolithic construction whereas the remainder of the external tank is of ring stiffened sheet construction, the sheet being thickened where large drag loads exist. The LH_2 tank is 2024 aluminum and the overall length is 4.27 m (168 in.). The chem-milled tank skin thickness is primarily 0.406 mm (0.016 in.) and typically increases to 0.635 mm (0.025 in.) in load carrying areas such as the orbiter interstage connections.

The solid rocket booster consists of a cylinder, a forward tank/SRB interstage, shown in figure 15, and an SRB aft skirt as shown in figure 19. The cylinder is 2024 aluminum and is approximately 3.7338 m (147 in.) long, 5.080 mm (0.2 in.) thick, and has a radius of 0.2477 m (9.75 in.).

A more complete description of the model design is presented in Reference 1. The significant structural dynamic characteristics to be represented in a model for various problem areas which are the basis for a model design are described in Reference 2.

ANALYTICAL MODELING PROCEDURE

Basic Philosophy

The entire vehicle has been analyzed by using NASTRAN. In setting up the model and analysis procedures the following guide lines were established:

(1) The model should be of sufficient refinement to adequately predict overall dynamic behavior. No attempt would be made to try to predict local panel motions.

(2) The detail of modeling should be of sufficient refinement to allow us to predict internal load distributions that would be adequate for a preliminary design of the structure. Although we had no intention of computing internal loads we considered the analysis to be representative of an actual prototype design situation and we were interested in how NASTRAN would blend into a design environment.

(3) The total structure would be analyzed by employing substructuring techniques to see how well this aspect of NASTRAN would blend into a design environment. NASTRAN could, in principle, of course handle the entire structure as a single unit, but we did not feel that this represented a realistic situation.

(4) Separate analyses of the LOX and SRB were performed to investigate the hydroelastic and viscoelastic capabilities of NASTRAN.

(5) The NASTRAN weight analysis capability was used to calculate the individual component and total weights for the nonfluid portions of the model. A supplementary weight check was conducted and the NASTRAN results adjusted where necessary. Structural grid points were used as dynamic mass points using Guyan reduction as required. This procedure differs from Grumman's usual practice, which is to establish a weights model independent of the structural model. By this approach, unit loads on the weights model mass points are then beamed to appropriate structural node points. The dynamic model is then the same as the weights model or is a subset of it. This procedure inherently results in a small dynamic model and additional reduction schemes are not necessary. The equivalent

reduction takes place in the beaming of the unit loads from the weights model to the structural model. This method was not used because it would have required more extensive alters to the NASTRAN rigid formats, it would not use NASTRAN weight analysis capability, and it would have produced basic mode data at non physical points which might hinder test correlation.

Overall Analysis Flow

A schematic diagram of the analysis flow is shown in figure 20. As indicated the Orbiter was divided into five substructures: fuselage, cargo doors, fin, wing, and payload. The external tank was divided into two substructures: the LOX tank and the aft portion of the external tank that consisted of the inter tank skirt, LH_2 tank and aft tank skirt. The solid rocket booster was handled as a single unit consisting of the forward skirt, propellant cylinder and propellant, and the aft skirt.

In the analysis each of the five Orbiter substructures was analyzed to produce reduced stiffness and mass matrices for selected dynamic points and interface attachment points. Modes for these components were then obtained with the interfaces held, the exception to this being the fuselage which was analyzed in a free-free state. This was done to aid in checking and to help understand the behavior of the combined vehicle. The five substructure stiffness and mass matrices were then merged to form total Orbiter mass and stiffness matrices. These matrices were again reduced by "freeing up" the substructure interface points to yield final stiffness and mass matrices that were used in the modal analysis.

As mentioned earlier, seperate analyses were run on the LOX tank and the SRB to study the hydroelastic capability of NASTRAN and to investigate the effect of the viscoelastic properties of the propellant on the damping characteristics of the SRB. In the overall flow the SRB matrices were first reduced and then merged with the Orbiter and external tank matrices to form a total Shuttle system of equations. The LOX tank was not reduced in this process.

The aft portion of the external tank was reduced, analyzed seperately, and merged with the other components in forming the total Shuttle system of equations.

Substructuring Procedure

The basic substructuring procedure for combining elements as presented in the NASTRAN User's Manual has been followed with some minor changes in the assumptions used, and with more extensive DMAP alters. These alters are written for both Rigid Format 3 which permits the use of more efficient eigenvalue analysis procedures while assembling the orbiter model and also for Rigid Format 7. The latter is required because the hydroelastic model of the LO$_2$ tank results in nonsymmetric mass and stiffness matrices which cannot be treated in Rigid Format 3. The viscoelastic properties of the propellant also are accurately represented in Rigid Format 7.

The analytical model is assembled in two phases. The flow diagram for the analysis is shown in figure 21. In the first phase, each substructure is analyzed and checked separately. The output from this phase is assembled onto a copy tape for the symmetric and antisymmetric cases and then coupled in Phase 2.

The following changes to the basic substructuring assumptions have been made in formulating this procedure:

Any external supports present are included in the Analysis Set (a-set).

Any zero stiffness degrees of freedom and symmetric or antisymmetric boundary constraints at the model plane of symmetry, are included in the Single Point Constraint Set. No other degrees of freedom are included in this set.

Masses which are associated with zero stiffness degrees of freedom will be lost unless these degrees of freedom are "beamed" to adjacent points using Multipoint Constraints.

The interface degrees of freedom may be sequenced differently and in different coordinate systems in any two substructures to be coupled. Multipoint Constraints are used to relate the appropriate degrees of freedom irrespective of local coordinate systems or initial sequencing.

Although the general theory presented in the NASTRAN User's Manual for substructuring is correct, it does not provide analysis checks at various critical points in the procedure. Structural plots provide analysis checks in this substructuring procedure but are not considered sufficient for verifying more than structural topology.

The following checks have been incorporated in the analysis by means of extensive DMAP alters:

A rigid body check is made in Phase 1 after the generation of the reduced stiffness and mass matrices. Temporary rigid body supports are included in the deck as SUPORT cards for this purpose.

The structural transformation matrices Gm, Go and D are used to generate equilibrium matrices for the various constraint sets except single point constraints. These equilibrium matrices represent resultants about a chosen origin due to unit applied loads at the appropriate degrees of freedom.

Provision is made to compute either free-free modes or free modes with the substructure held at the interface. This is necessary if each substructure is to be checked independently in Phase 1.

A rigid body mass matrix relative to the basic origin is computed and compared with the general mass matrix calculated by the Grid Point Weight Generator. This check verifies that no mass has been lost in the reduction process.

The DMAP statements to perform these functions for Rigid Format 3 are presented in the Appendix.

Finite Element Model

The number of grid points and elements used in the five Orbiter substructures are shown in table 1. The fuselage shell structure was modeled using CQDMEM2 elements, a new element in NASTRAN but one that has been used widely at Grumman. It is essentially a quadrilateral that is composed of four triangles which have a common central node defined by the intersection of lines that connect the midpoints of the opposite sides of the quadrilateral. The four corner nodes need not lie in a plane. The fuselage U frames (see figures 4 and 5) and keel were idealized using CROD and CSHEAR elements. Here effective cap areas were calculated for the CROD elements to represent the appropriate bending behavior. CBAR elements with appropriate offsets were used to represent thin ring type frames such as the engine compartment closure frame (see figure 2).

The webs in the wing ribs and spars (see figures 6, 7, and 8) were idealized with CSHEAR elements. Again the effective rib and spar bending material was incorporated into CROD elements in the upper and lower covers. The covers themselves were represented by CQDMEM2 elements and some CTRMEM elements that occur at the leading edge. Intermediate node lines that lie between the spar and rib node lines were established to further refine the grid used in the covers. The geometry of these lines is essentially set by the location of fuselage frames.

The idealization of the fin follows closely the same scheme used in the wing (see figures 9 and 10).

The shell portion of the cargo bay door (figure 11) was idealized using CQDMEM2 elements with the exception of a few CQUAD2 elements that were required for local stability to provide an attachment point of the doors to the fuselage. The door frames were idealized as CSHEAR and CROD elements. Note that these frames contain two webs (figure 12), one common lower cap, and two upper caps that connected to the forward and aft shell segments. This allows the doors to "breath" in longitudinal direction.

Although provision was made for testing four payload configurations, the analysis included only one that represented the full up payload of 289 kN (65 000 lb). The stiffened box section payload was represented by a series of CBAR elements. The payload is shown mounted in the fuselage in figure 2.

The fluid in the LOX tank was represented by a network of four concentric fluid rings, 13 levels deep. The shell was idealized as CQUAD2 and CTRIA2 plates while the Y-ring was represented by CBAR elements. The shell was divided into $22\frac{1}{2}^{\circ}$ segments in the circumferential direction and 17 stations in the meridional direction.

The aft portion of the external tank (figure 13) was modeled using CQUAD2 elements to represent the shell. Double frames exist at the forward and aft portions of the inter tank skirt and an additional longitudinal node line is picked up in this region to account for the SRB drag attachment and the stiffening that exists in the shell. Five heavy frames exist in the aft external tank; the first at STA 99.98 which is the forward tank/SRB interstage; the second at STA 148.756 which is the orbiter forward interstage; the third and fourth at stations 229.156 and 245.7536 which pick up the orbiter aft interstage fitting; and the fifth at station 270.988 which is the aft tank/SRB interstage.

These heavy frames have internal struts to provide additional stiffening to the interstage attachment points (figure 18). The remainder of the frames are light and are included to prevent shell buckling. In the prototype design, the real shell was stiffened in the longitudinal direction. In the model this stiffening plus the skin thickness was lumped to yield an effective thickness which was then scaled to the dimensions of the 1/8-scale model. This was done for the sake of economy in constructing the 1/8-scale model.

The solid rocket booster finite element idealization consists of CQUAD2 plate elements (containing membrane and bending properties) to represent the skin, straps, and plates; three-dimensional elements to represent the propellant; and offset bar elements to represent the frames and longerons. A NASTRAN generated plot of the outer shell is shown in figure 22 along with the frame stations. The thickness of the forward skirt varies from 1 to 6 mm (0.040 to 0.230 in.), the propellant cylinder thickness is 5 mm (0.1875 in.) and the aft skirt thickness is 2 mm (0.062 in.). The propellant is modeled by three layers (in the radial direction) of three-dimensional elements whose properties are $E^1 = 172.37$ MN/m^2 (25×10^3 psi), $\nu = 0.49$, $\rho = 1716.15$ kg/m^3 (0.062 lb/in^3) and a structural damping factor $\beta = 0.52$ where $\beta = G''/G' = E''/E'$ ($E = E' + E11$, $G = G' + G''$). The total weight of the structure and propellant is 11 kN (2520 lb).

ANALYTICAL RESULTS

Orbiter Component Analysis

The analysis of the separate components conducted as part of Phase 1 is used to establish confidence in the finite element models at that level. The NASTRAN generated weights were compared with those determined independently and discrepancies were rectified. The vibration eigenvalues and eigenvectors were calculated for the components restrained at their supports, or free, whichever seemed most applicable. These were examined and any departure from anticipated results was investigated. This check helped uncover problems in the way constraints were specified and some other data difficulties. The lowest frequency modes obtained during these component analyses were as follows:

Fuselage:			
Free, symmetric	62.2 Hz	129.9 Hz	
Free, antisymmetric	89.1 Hz	128.3 Hz	
Payload:			
Restrained, symmetric	81.2 Hz	268.5 Hz	627.7 Hz
Restrained, antisymmetric	68.6 Hz	175.4 Hz	462.8 Hz
Cargo doors:			
Free, symmetric	4.6 Hz	10.7 Hz	17.6 Hz
Restrained, antisymmetric	156.4 Hz	622.2 Hz	1054.6 Hz
Wing:			
Restrained	77.6 Hz	158.3 Hz	259.9 Hz
Fin:			
Restrained, symmetric	264.2 Hz	841.3 Hz	1263.3 Hz
Restrained, antisymmetric	107.8 Hz	407.2 Hz	1018.7 Hz

Total Orbiter Analysis

After the individual components were analyzed, the entire orbiter vehicle was coupled and a vibration analysis was performed in Rigid Format 3. PLOTEL elements were used to connect the grid points retained for plotting purposes. In order to examine the deformation more readily, both a side view and a bottom view were plotted for each mode. Only the latter includes the payload. The deformed shape was plotted together with the X, Y, and Z vectors from the underformed location. The first two elastic modes are shown in figures 23 to 26. The first mode at 53.0 Hz exhibits fuselage vertical bending, fin pitching, and wing motion. Wing motion appears to be due to flexibility in the root restraint and the deformed shape is almost a straight line. The maximum motion point is at the fin tip and results from pitching of the back part of the model. The second elastic mode at 62.6 Hz is principally wing bending with some payload and fuselage vertical bending.

Initial comparisons with test data indicate that there is more flexibility in the fin and wing attachment in the physical model than was allowed for in the analyses. The orbiter finite element model is readily adapted to exploring these effects and several runs were made varying the fin attachment. Results showed that the aft frame in the orbiter offers little stiffness to the aft fin spar in the vertical direction, but the forward frames are very significant. The first symmetric mode calculated with the forward frame vertical forces eliminated from the NASTRAN model is shown in figures 27 and 28. The frequency dropped from 53.0 to 48.0 and the relative deformation of the fin is easily noted.

LO_2 Tank Analysis

The full LO_2 tank model, with no omits, was analyzed for the zeroth and first harmonics only for the frequency range from 8 Hz to 135 Hz. This frequency range was selected to avoid calculating the slosh modes which were not considered significant in our analysis. The modes obtained can be most readily characterized by the variation in pressure.

SUMMARY OF HYDROELASTIC MODES

[1/8-scale LO_2 tank]

Frequency, Hz	Characteristic pressure pattern
Zeroth pressure harmonic (circumferential pressure = cos 0θ)	
22.9	No nodal surfaces
75.2	1 node at about midtank
91.5	2 nodes
115.2	3 nodes
First pressure harmonic (circumferential pressure = cos 1θ)	
19.2	No nodal surfaces
60.5	1 node
110	2 nodes
134.3	3 nodes

The corresponding grid point deformation for the original structural idealization indicated irregularities associated with the finite element model of the lower dome. Since the pressure gradations in the lower hydroelastic modes were relatively uniform, it appears suitable to investigate the effects of dome finite element size and geometry using static pressure loading to save computer time. The static loading produced deformations very similar to those in the fundamental hydroelastic modes. One modification attempted, the use of membrane elements in place of plate elements, gave no appreciable improvement. The original finite element grid was then refined by adding more elements, and the geometry was corrected. The resulting deformation pattern was considered acceptable. The current version of the tank dome finite element representation is shown in figure 29. Both the undeformed shape and the pattern under a uniform pressure of 6.9 kN/m^2 (1 psi) are shown.

External Tank Analysis

In assembling the external tank model, the LH_2 tank including the skirts at both ends was analyzed as an empty free shell. Vibration modes resulting from these computations indicated that above the first bending mode at 139.2 Hz, the modes of the central portion of the LH_2 tank in the areas of the light frames exhibited radial deformation typical of shell modes in cylinders.

An interesting comparison of the NASTRAN calculated weights and those determined independently by a weights engineer is as follows:

Tank weight as calculated from structural drawings, including fittings, fasteners, etc.	603.2 N	(135.6 lb)
Finite-element model weight (twice the half tank weight)	589.4 N	(132.5 lb)
c.g. position aft of forward dome as calculated by weights engineer	1.901 m	(75.14 in.)
c.g. position as calculated by NASTRAN for the finite element model	1.912 m	(75.29 in.)

The weight of the LH_2 is distributed as nonstructural mass in the CQUAD2 and CTRIA2 elements.

After the LH_2 tank model is checked, it is reduced and coupled with the LO_2 model. Analysis for this coupled structure has not yet been completed.

SRB Analysis

In order to obtain a guide for the finite element idealization of an empty tank, the SRB was modeled as a cylinder of radius 0.25 m (10 in.) and length 5.08 m (200 in.). The finite element idealization consisted of 21 bays along the length and 12 bays around the circumference. The following table represents a comparison of results between NASTRAN using the Givens method, Grumman's STARS-2V program, and NASA Langley's SRA program (refs. 3 and 4, respectively). The STARS-2V and SRA programs are based on thin-shell orthotropic theory. The accuracy of the NASTRAN results are relatively good for the lower modes and depend upon the relative complexity of the eigenvectors.

EMPTY CYLINDER VIBRATION ANALYSIS

Frequency, Hz			
STARS-2V	SRA	NASTRAN (householder method)	% Error
52.0 (n=2, 1st)	51.56 (n=2, 1st)	55.2	6
52.4 (n=2, 2nd)	51.66 (n=2, 2nd)	54.9	5
66.6 (n=2, 3rd)	66.04 (n=2, 3rd)	73.9	11
119.3 (n=1, 1st)	120.16 (n=1, 1st)	122.5	3
120.4 (n=2, 4th)	--	171.8	42
147.1 (n=3, 1st)	--	165.1	12

The undamped vibrational modes for the full cylinders are tabulated in the tables that follow. The modes of most interest are the 1st and 2nd bending modes and the longitudinal rod and thickness shear mode. Figures 30(a) and 30(b) show cross sectional views of the vibrational motion, and figures 31(a), 31(b), and 31(c) show orthographic views of the motion obtained from the NASTRAN analysis. The first table also includes the results for simple beam theory for the modes of interest (bending and longitudinal) based on the composite properties of the tank. Using a structural damping factor of 0.52 for the propellant elements, the complex eigenvalues for the lowest bending and longitudinal modes were obtained (Rigid Format 7) and compared with the undamped modes as tabulated in the second table. Simple beam theory (no shear) predicts a value of $1/Q = 0.028$, which agrees with the bending mode. The difference between this value and that for the longitudinal mode is due to the thickness shear effects. (See figure 30(b).) It was found that the damped vibrational analysis was run more efficiently by analyzing the undamped system first in order to narrow the search range. However, computer running times were still quite long.

VIBRATION ANALYSIS OF FULL PROPELLANT CYLINDER

Mode	Frequency, Hz	
	NASTRAN	Simple beam theory
n=1, m=1	56.4	58.4
n=0, torsion	171.4	
n=1, m=2	173.0	161.0
n=0, longitudinal	196.1	180.2

VIBRATION ANALYSIS USING DAMPED SOLID FINITE ELEMENTS

Mode	Frequency, Hz		Damping value, 1/Q (a)
	Undamped	Damped	
Bending - 1st	56.38	56.39	0.027
Longitudinal - 1st	196.0	197.1	.056

[a] $1/Q = \eta$ where η is the equivalent damping constant; c.f., Tong, Kin N.: Theory of Mechanical Vibrations. John Wiley & Sons, Inc., 1960, p. 15.

Total Vehicle Analysis

At the time of this writing, vibration analysis results for the completely coupled shuttle configuration were not available.

NASTRAN EXPERIENCES

Hydroelastic Analysis

Some difficulties were encountered in attempting to run the hydroelastic analysis. Before setting up the 1/8-scale model LO_2 tank, the program was run for a small problem containing 86 degrees of freedom in the analysis a-set. After this had been run successfully, the LO_2 tank which had 717 a-set degrees of freedom, was modeled and submitted for computation. A summary of the difficulties encountered conducting the larger hydroelastic analysis are as follows:

(a) Hydroelastic problems will not run in Level 15-5 of NASTRAN. A system ØC1 error occurs while executing module GKAD. This error has been reported to NSMO and is listed as SPR [illegible].

(b) Often only a single Eigenvalue is extracted, using the Inverse Power Method, although more are present. This we now feel is a function of incorrect completion codes. This error is now listed as SPR 995.

(c) Fluid rings must be input in ascending order on RINGFL cards or program terminates with error No. 2001. This error has been reported to NSMO and is listed as SPR 1017.

(d) Fluid element identification numbers are limited in size to approximately 30 000 or less. Numbers greater than this cause a ØC5 system error in Module TA1. This error is now listed as SPR 1016.

(e) BAROR card causes fatal error in hydroelastic analysis. This error has been reported to NSMO.

(f) Data block M_{AA} is not pooled correctly in module SMP2 in Level 15.1. This causes fatal error 1105 if program is checkpointed. (Problem runs without checkpoint). This error has been reported to NSMO.

One continued difficulty was the large amount of computer running time required for the eigenvalue solutions in Rigid Format 7.

No information is available either in the literature or from NSMO regarding the reduction of the number of D.O.F. when using fluid elements in hydroelastic problem. And yet, if shuttle hydroelastic analyses are to be accomplished in moderate computer time then a major reduction seems advisable. In order to determine if such a reduction is possible, a small hydroelastic problem was used. It was found that using the internally generated fluid point numbers on OMIT cards did not violate any NASTRAN rules and the program ran successfully to completion. These internal numbers may be calculated following the rules in the NASTRAN User's Manual or an unreduced problem may be run as far as GP4 with diagnostic 21 turned on.

A review of the frequencies shown in the following table indicates that the results are comparable for the lower frequency modes.

EFFECT OF REDUCING FLUID POINTS IN HYDROELASTIC ANALYSIS

[Simple 1/8-segment of hemispherical tank,
total degrees of freedom = 154]

Mode	Frequency, hz	
	No omitted points analysis D.O.F. = 85	Omitted fluid points analysis D.O.F. = 77
1	283	292
2	421	436
3	536	544
4	606	698
5	697	797

SRB Analysis

For the empty propellant cylinder the inverse power method found erroneous roots and left out some roots. These roots were subsequently found using the Givens method and the erroneous roots did not appear. The Givens method generally did not work for large problems on level 15.5 but did work on level 15.1. The damped vibrational analysis, using Rigid Format 7, gave a fatal error message after finding the eigenvalues. The eigenvalue running times tended to be long (1000 CPU seconds on an IBM 370/165 for 176 reduced D.O.F. using the DET method). These errors did not occur for very small prototype problems. Other difficulties that were encountered included erroneous fatal messages; for example, a U602 message was encountered for a singular matrix. These errors also seemed to be a function of the large size problems under consideration.

Orbiter Coupling Analysis

Once the DMAP alters were debugged, essentially no major problems were encountered as far as obtaining results for the orbiter. The incorporated checks and plots proved to be major aides in "debugging" the input data to Phase 1. Experience with the various alters is listed below:

(1) Incorporating the rigid body checks in phase 1 is essential in determining if there are any erroneous constraints in the substructures.

(2) If the rigid body check is not satisfactory and the erroneous constraint is limitted to a single constraint, then printing the reduced rigid body support stiffness $[X]$ and obtaining from it the resultants of the rigid body forces helps in locating the coordinates of the erroneous constraint.

(3) If the trouble is caused by MPC's then the resultants of the m-set loads helps in locating MPC errors.

(4) If MPC's and SPC's are in error, mode plots are helpful in locating erroneous SPC's and sometimes MPC's.

(5) If free-free modes are obtained, then printing the member forces and/or SPC forces for the rigid body modes may help in locating the erroneous constraint since the structure should be free of stress.

(6) Mode plots in phase 1 have helped in determining whether the appropriate nodes have been selected as dynamic degrees of freedom. In some cases "soft spots" were accidentally selected for the a-set and these caused local motions to show up in the mode plots.

In order to obtain plots in the coupling run (phase 2) it is suggested that grid points rather than scalar points be used in the coupling phase. PLOTEL elements were then used to connect the grid points creating a pseudostructure that is suitable for plotting. The grid points established in phase 2 were the grid points that are associated with the substructure a-set degrees of freedom. All non-strainable D.O.F. were removed by SPC's. It should be noted that each substructure had a unique grid point numbering system so that the grid cards in the a-set of each substructure could be duplicated and incorporated in phase 2. Common interface points were made common by MPC's.

If necessary the a-set of a given substructure was increased so that a more realistic plot could be obtained. This also necessitated having x, y, and z D.O.F. at all points to be plotted so that all significant motion is displayed.

To prevent loss of mass, it is recommended that mass should not be assigned to grid points having nonstrainable D.O.F., such as, intermediate grid points in a planar frame. If assigning mass to such nodes is necessary, then MPC's should be used instead of SPC's to remove the singularity from the stiffness matrix; this will conserve the total mass distribution.

System Experience

One of the fallouts of our analysis of the 1/8-scale model has been a further evaluation and demonstration of the program that is scheduled to eventually replace our own in-house system. Partly as a result of this work, we believe that NASTRAN is ready to handle the analysis of large aerospace vehicles such as the shuttle. We would like to point out, however, some additional features associated with NASTRAN which must be given consideration.

(1) The learning curve for NASTRAN is rather flat. If you want to be in a position of making extensive alters to the rigid formats, and any aerospace company faced with large complex problems must be in this position, then the investment in learning time is large. Future levels of NASTRAN should concentrate on building a system that is more easily altered. We feel that it is far more important to devote NASTRAN funds to developing a sound basic system than to adding capability for solving specialized problems.

(2) Our in-house developed postprocessor for converting selected NASTRAN element corner forces, for example, membrane elements and rod-shear panel assemblies, has been completed (available from level 15.5). Although not used on the 1/8-scale model analysis this program is a necessity if we are to obtain internal member loads in a form required by our designers.

(3) Experience in running large problems in NASTRAN should be established prior to actual run submissions. Adequate time should be provided for difficulties encountered the first few times a new problem is run. The availability of experienced computer systems analysts capable of assisting in such difficulties helps materially in expediting NASTRAN analyses.

ACKNOWLEDGEMENT

We would like to thank the members of the Vibration Section, Structures and Dynamics Division, Langley Research Center, for their guidance and assistance in the work described herein.

REFERENCES

1. Grumman Aerospace Corp.: Design of a Space Shuttle Structural Dynamics Model. NASA CR-112205, [1973].

2. Grumman Aerospace Corp.: Preliminary Shuttle Structural Dynamics Modelin Design Study. NASA CR-112196, Nov. 1972.

3. Svalbonas, V.: Numerical Analysis of Stiffened Shells of Revolution - Theory Manual for STARS-2S, -2B, -2V Programs. IOM 000-STMECH-038, Grumman Aerospace Corp., May 10, 1973.

4. Cohen, Gerald A.: User Document for Computer Programs for Ring-Stiffened Shells of Revolution. NASA CR-2086, 1973.

APPENDIX

NASTRAN SUBSTRUCTURING ANALYSIS FOR NORMAL MODES

ALTERED RIGID FORMAT 3 FOR PHASE 1 OR 2

Incorporated New Bulk Parameters

(1)	NOSUB	Number of substructures to be coupled in this run. Default = 1, which indicates a phase 1 run, where one substructure will be reduced.
(2)	TPCOPY≥0	Will put reduced stiffness and mass matrix (Kaa & Maa) on tape INPT. Default = -1
(3)	TPNAME	Label name of INPT. Use only when TPCOPY≥0
(4)	RMODE≥0	Causes restrained free modes to be obtained. The restraints are defined in an input column partition matrix [CPAJC], which will partition the a-set into J & C sets. Default = -1. In this case free-free modes will be obtained if there is a SUPORT card in the BULK data, defining the rigid body supports. Although [CPAJC] is not used when RMODE = -1, it must be defined in the BULK data. It is sufficient to define it as a 1 × 1 matrix. Also, don't forget the EIGR card if modes are to be obtained.
(5)	TPNAME9	Label name of INP9, which contains the column partition vector, reduced stiffness, and mass for each reduced substructure. The column partition vectors are used to merge the reduced stiffness and mass of each reduced substructure into a common pseudo-structure lineup. Use this parameter only when NOSUB>1.
(6)	TPCOPYN≥0	Will put the pseudostructure eigenvalues and eigen-vectors in substructure lineups on tape (INP1, INP2, etc.) for further processing, in this case final substructure mode shapes. Default = -1.
(7)	TPNAMEN	Common label name of INP1, INP2, etc. Use only when TPCOPYN≥0.

Incorporated New Bulk Input Matrices

The following input matrices must be defined in the BULK data on DMI cards whether they are needed or not. If they are not needed, defining them as a 1 × 1 matrix will suffice.

(1) EQR Matrix

This matrix expresses the resultants about an origin, due to unit rigid body support loads. The rigid body degrees of freedom are defined on the standard NASTRAN SUPORT card. The EQR matrix is necessary if the checks, which are incorporated in the ALTERS, are to be performed. The origin chosen, should be the same origin defined on the standard GRDPNT parameter card.

(2) CPAJC Matrix

This matrix is used when restrained-free modes are to be obtained (RMODE=1). This matrix is a column partitioning vector which defines the restrained degrees of freedom from the analysis set (a-set) degrees of freedom.

IMPORTANT NOTE:

When doing a coupling run, where all substructures have been reduced and on tape, it was necessary to input in the BULK data at least one element, to prevent a fatal error in module TA1. A thin, string-like rod will suffice. The element must be counted as a substructure so that the new NOSUB parameter was increased by one.

Alters Incorporated (General Flow)

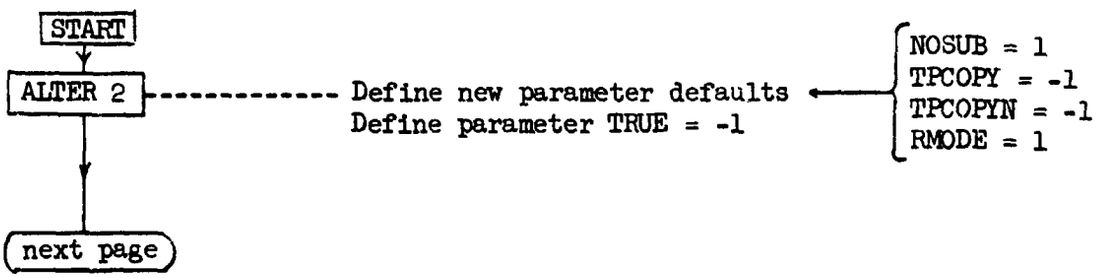

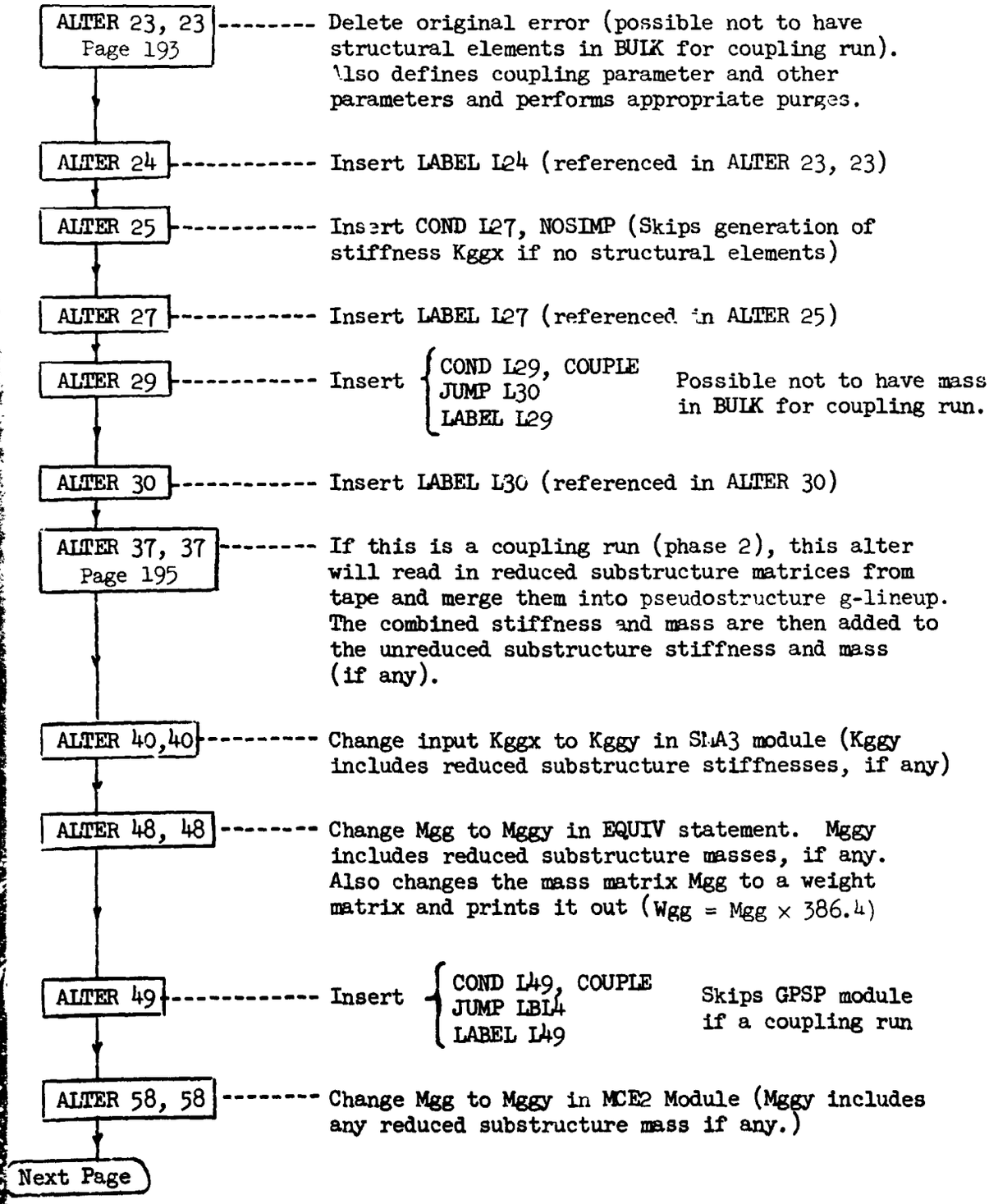
ALTER 23, 23
Page 193
Delete original error (possible not to have structural elements in BULK for coupling run). Also defines coupling parameter and other parameters and performs appropriate purges.
ALTER 24
Insert LABEL L24 (referenced in ALTER 23, 23)
ALTER 25
Insert COND L27, NOSIMP (Skips generation of stiffness Kggx if no structural elements)
ALTER 27
Insert LABEL L27 (referenced in ALTER 25)
ALTER 29
Insert
COND L29, COUPLE
JUMP L30
LABEL L29
Possible not to have mass in BULK for coupling run.
ALTER 30
Insert LABEL L30 (referenced in ALTER 30)
ALTER 37, 37
Page 195
If this is a coupling run (phase 2), this alter will read in reduced substructure matrices from tape and merge them into pseudostructure g-lineup. The combined stiffness and mass are then added to the unreduced substructure stiffness and mass (if any).
ALTER 40,40
Change input Kggx to Kggy in SMA3 module (Kggy includes reduced substructure stiffnesses, if any)
ALTER 48, 48
Change Mgg to Mggy in EQUIV statement. Mggy includes reduced substructure masses, if any. Also changes the mass matrix Mgg to a weight matrix and prints it out (Wgg = Mgg × 386.4)
ALTER 49
Insert
COND L49, COUPLE
JUMP LBL4
LABEL L49
Skips GPSP module if a coupling run
ALTER 58, 58
Change Mgg to Mggy in MCE2 Module (Mggy includes any reduced substructure mass if any.)
Next Page

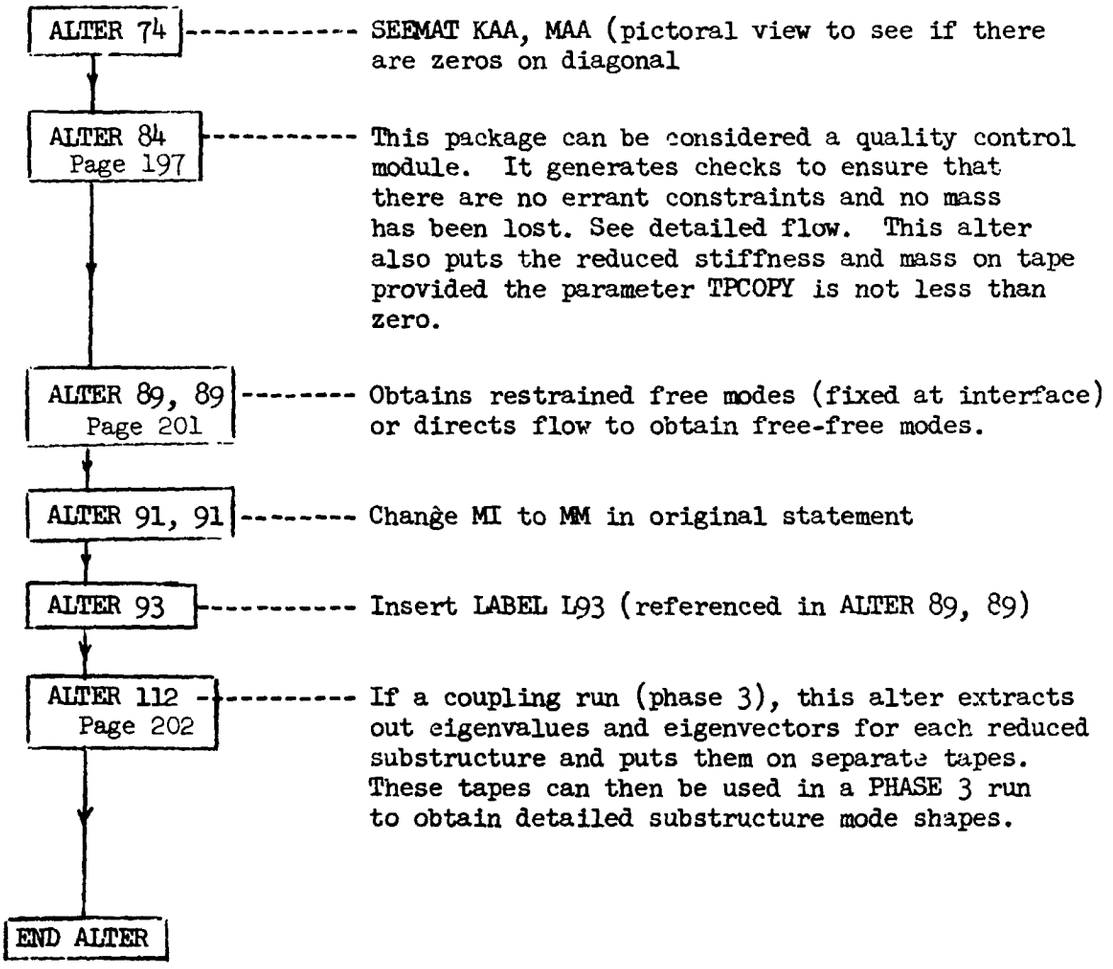
ALTER 74
SEEMAT KAA, MAA (pictoral view to see if there are zeros on diagonal
ALTER 84
Page 197
This package can be considered a quality control module. It generates checks to ensure that there are no errant constraints and no mass has been lost. See detailed flow. This alter also puts the reduced stiffness and mass on tape provided the parameter TPCOPY is not less than zero.
ALTER 89, 89
Page 201
Obtains restrained free modes (fixed at interface) or directs flow to obtain free-free modes.
ALTER 91, 91
Change MI to MM in original statement
ALTER 93
Insert LABEL L93 (referenced in ALTER 89, 89)
ALTER 112
Page 202
If a coupling run (phase 3), this alter extracts out eigenvalues and eigenvectors for each reduced substructure and puts them on separate tapes. These tapes can then be used in a PHASE 3 run to obtain detailed substructure mode shapes.
END ALTER

ALTER 23,23 DETAILED FLOW

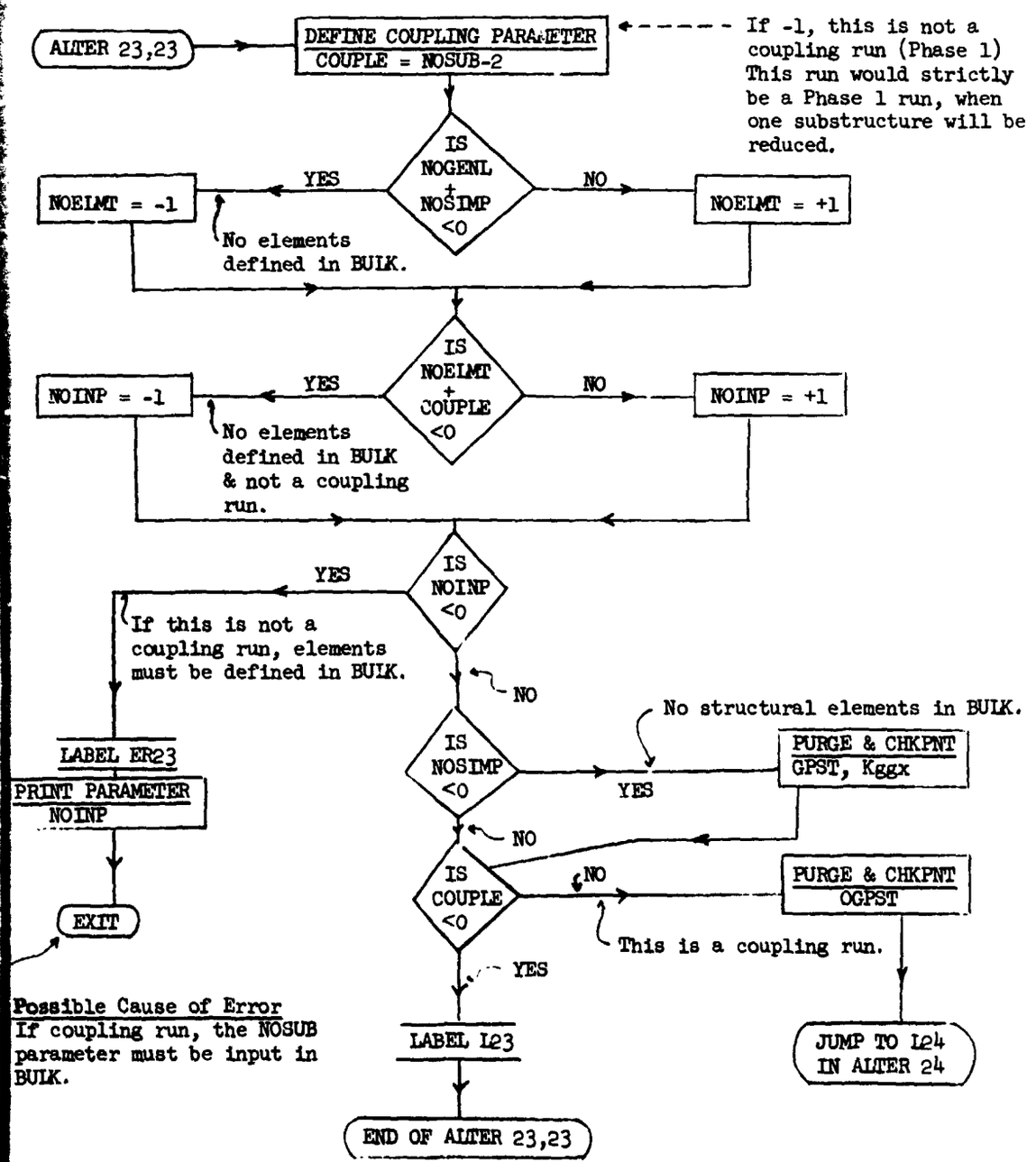

ALTER 37, 37 DETAILED FLOW

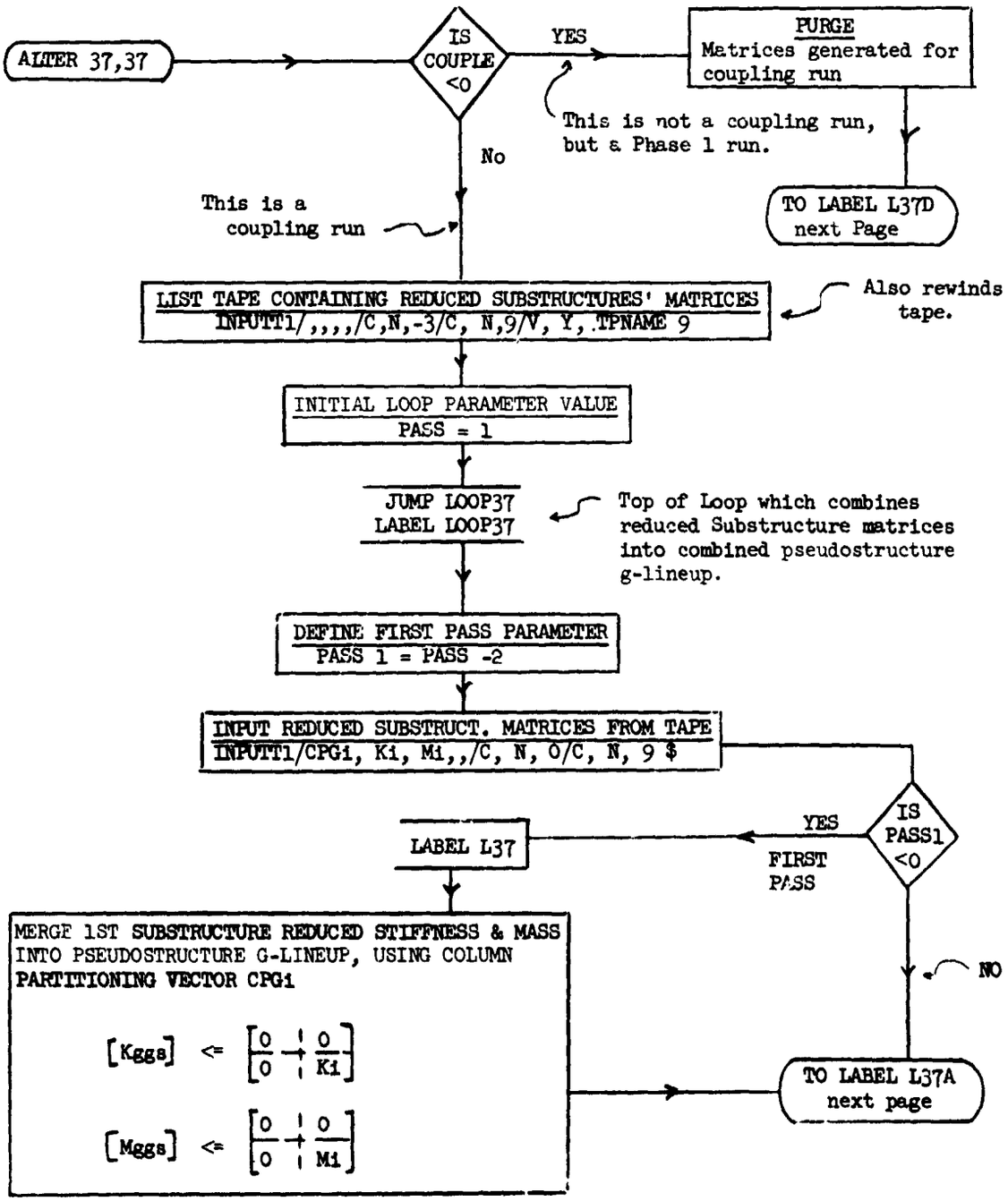

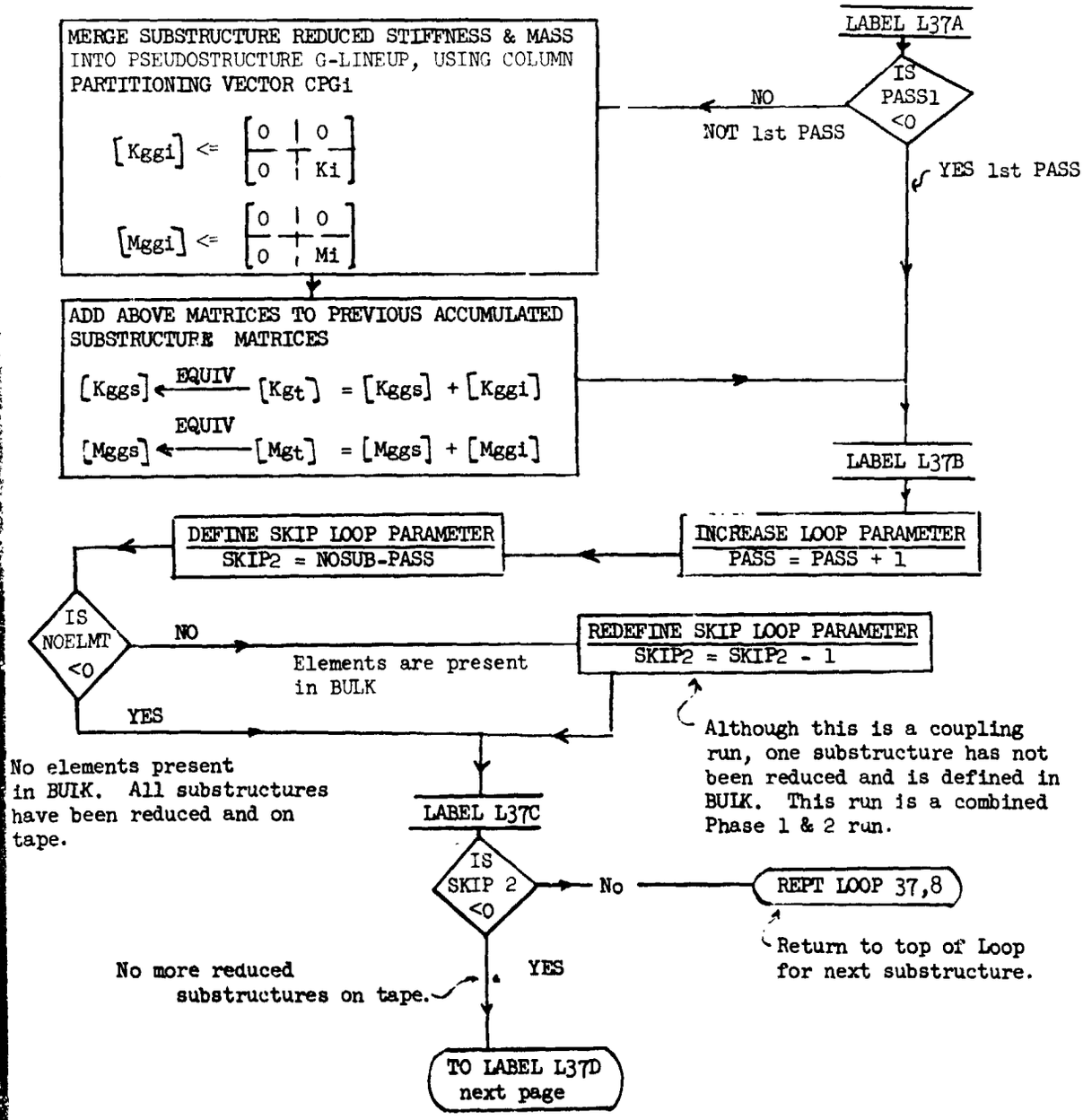
MERGE SUBSTRUCTURE REDUCED STIFFNESS & MASS INTO PSEUDOSTRUCTURE G-LINEUP, USING COLUMN PARTITIONING VECTOR CPGi
[Kggi] <= [0 | 0 / 0 | Ki]
[Mggi] <= [0 | 0 / 0 | Mi]
ADD ABOVE MATRICES TO PREVIOUS ACCUMULATED SUBSTRUCTURE MATRICES
[Kggs] EQUIV <- [Kgt] = [Kggs] + [Kggi]
[Mggs] EQUIV <- [Mgt] = [Mggs] + [Mggi]
LABEL L37A
IS PASS1 <0
NO
NOT 1st PASS
YES 1st PASS
LABEL L37B
INCREASE LOOP PARAMETER
PASS = PASS + 1
DEFINE SKIP LOOP PARAMETER
SKIP2 = NOSUB-PASS
IS NOELMT <0
NO
Elements are present in BULK
REDEFINE SKIP LOOP PARAMETER
SKIP2 = SKIP2 - 1
Although this is a coupling run, one substructure has not been reduced and is defined in BULK. This run is a combined Phase 1 & 2 run.
YES
No elements present in BULK. All substructures have been reduced and on tape.
LABEL L37C
IS SKIP 2 <0
No
REPT LOOP 37,8
Return to top of Loop for next substructure.
No more reduced substructures on tape.
YES
TO LABEL L37D next page

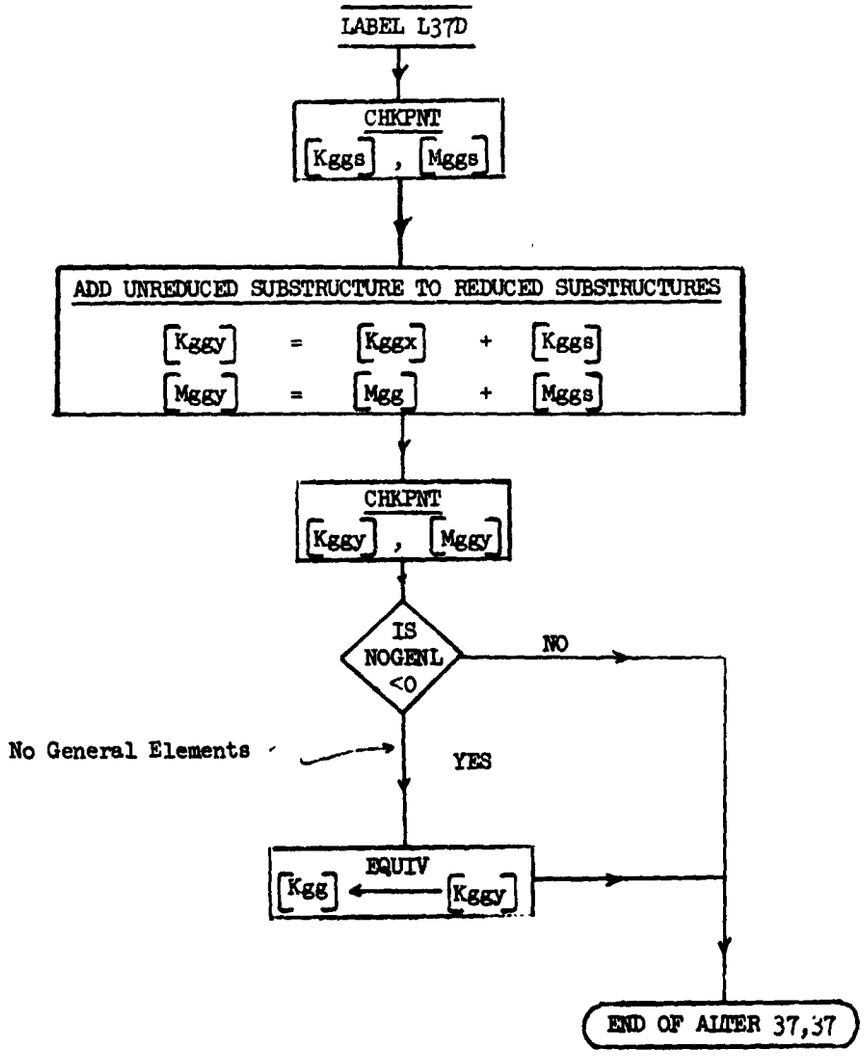
LABEL L37D
CHKPNT
[Kggs] , [Mggs]
ADD UNREDUCED SUBSTRUCTURE TO REDUCED SUBSTRUCTURES
[Kggy] = [Kggx] + [Kggs]
[Mggy] = [Mgg] + [Mggs]
CHKPNT
[Kggy] , [Mggy]
IS NOGENL <0
NO
No General Elements
YES
EQUIV
[Kgg] [Kggy]
END OF ALTER 37,37

ALTER 84 DETAILED FLOW

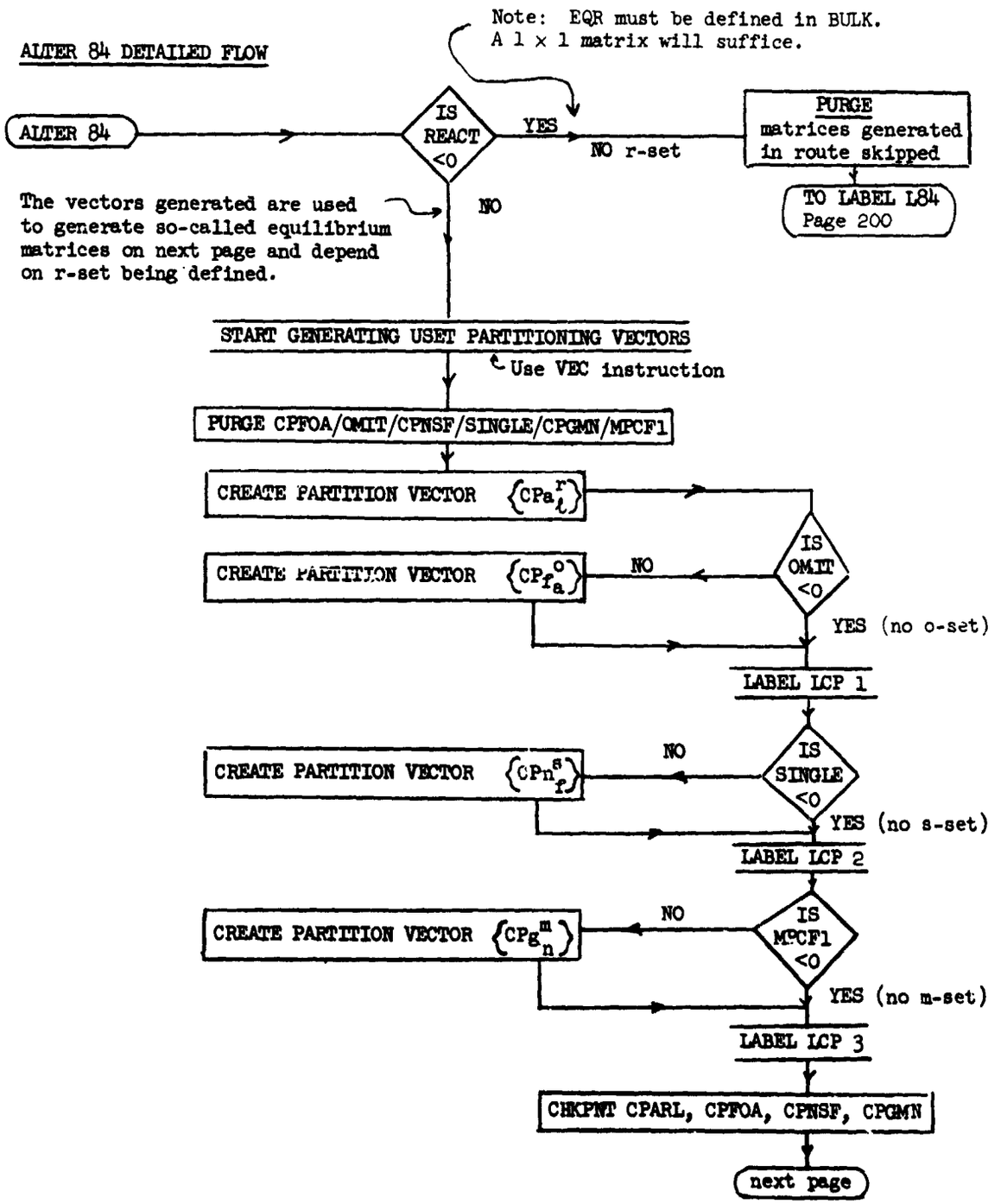

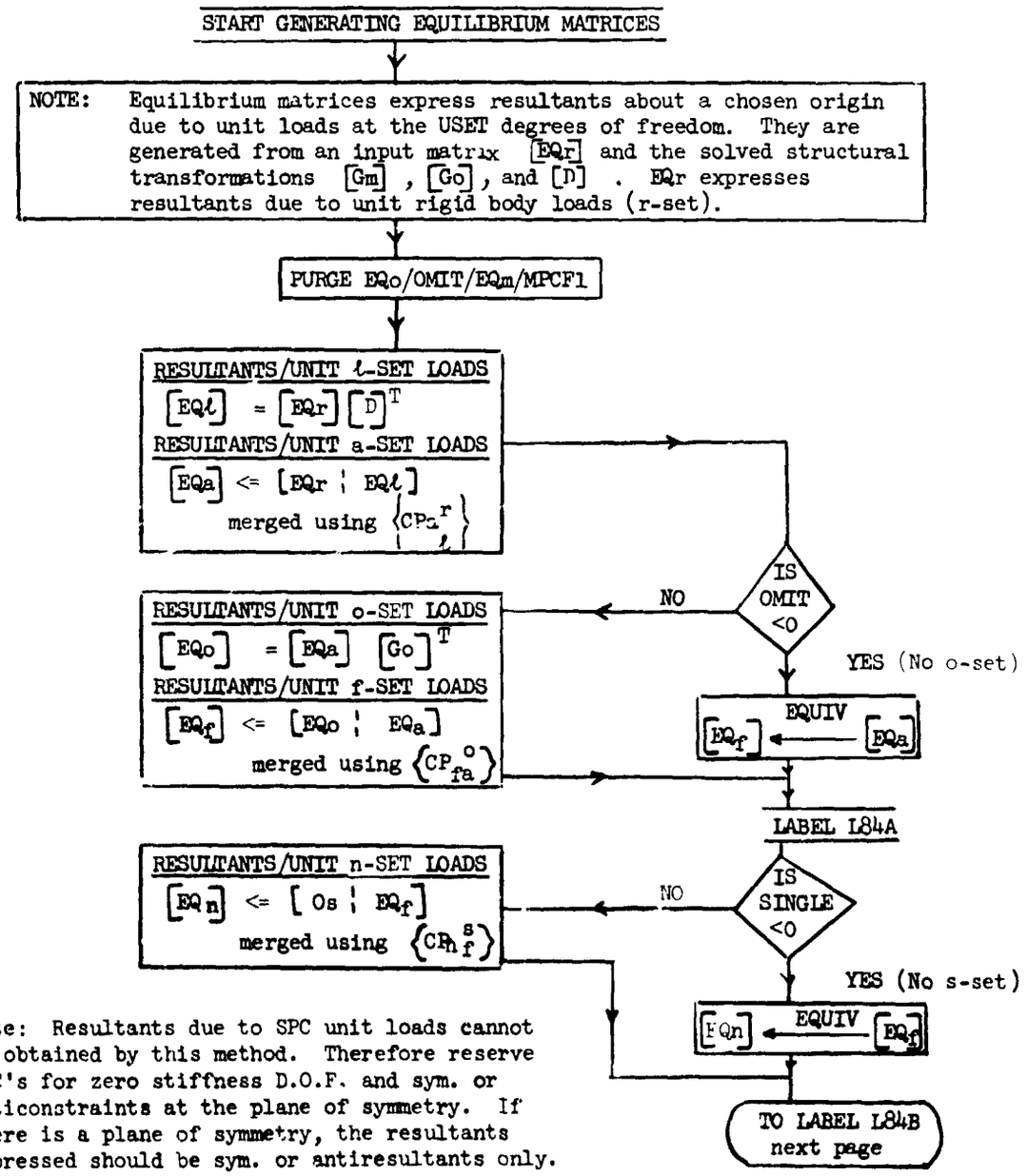

Note: Resultants due to SPC unit loads cannot be obtained by this method. Therefore reserve SPC's for zero stiffness D.O.F. and sym. or anticonstraints at the plane of symmetry. If there is a plane of symmetry, the resultants expressed should be sym. or antiresultants only.

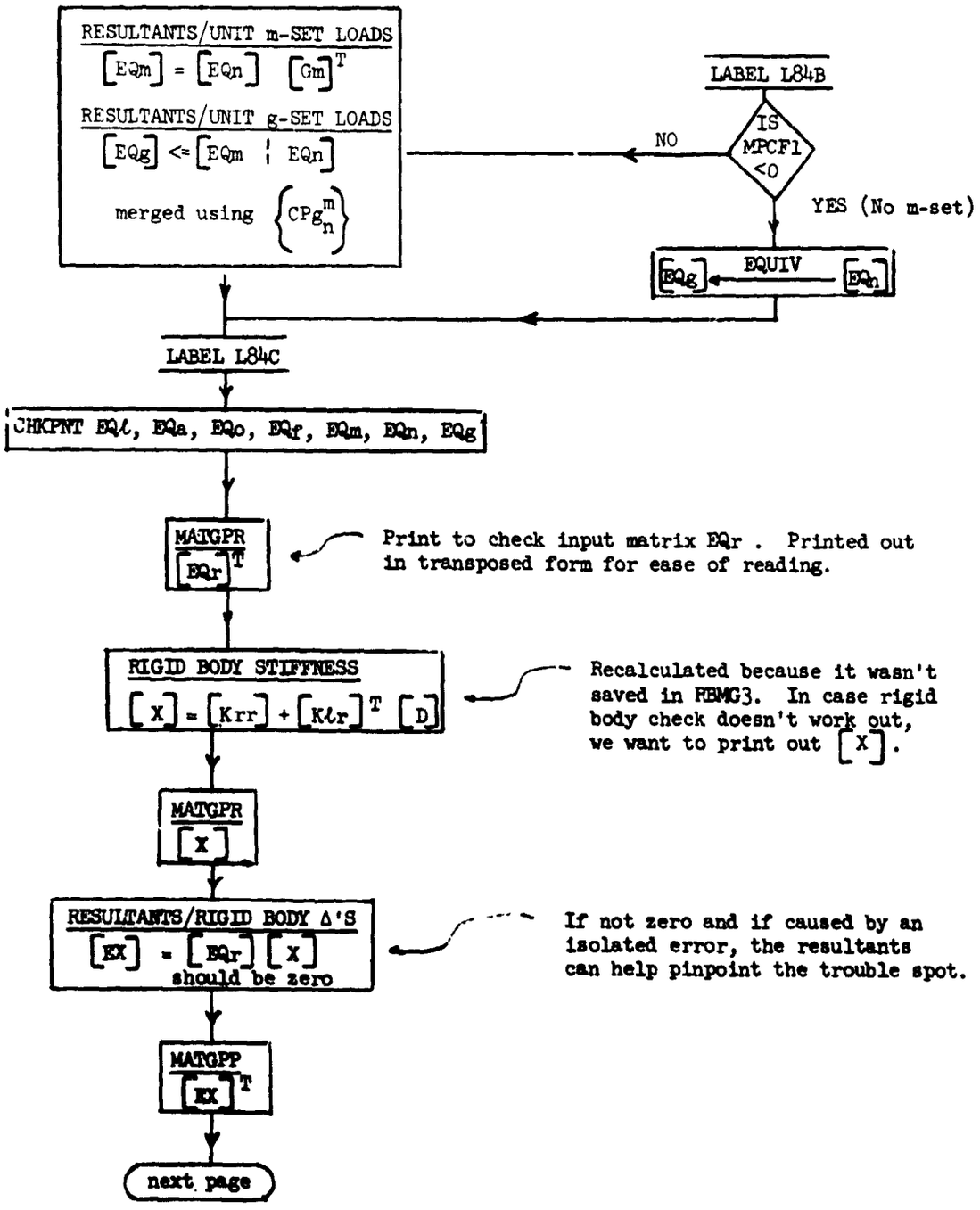
RESULTANTS/UNIT m-SET LOADS
[EQm] = [EQn] [Gm]T
RESULTANTS/UNIT g-SET LOADS
[EQg] <= [EQm ¦ EQn]
merged using {CPgnm}
LABEL L84B
IS MPCF1 <0
NO
YES (No m-set)
[EQg] EQUIV [EQn]
LABEL L84C
CHKPNT EQℓ, EQa, EQo, EQf, EQm, EQn, EQg
MATGPR [EQr]T
Print to check input matrix EQr . Printed out in transposed form for ease of reading.
RIGID BODY STIFFNESS
[X] = [Krr] + [Kℓr]T [D]
Recalculated because it wasn't saved in RBMG3. In case rigid body check doesn't work out, we want to print out [X].
MATGPR [X]
RESULTANTS/RIGID BODY Δ'S
[EX] = [EQr] [X]
should be zero
If not zero and if caused by an isolated error, the resultants can help pinpoint the trouble spot.
MATGPP [EX]T
next page

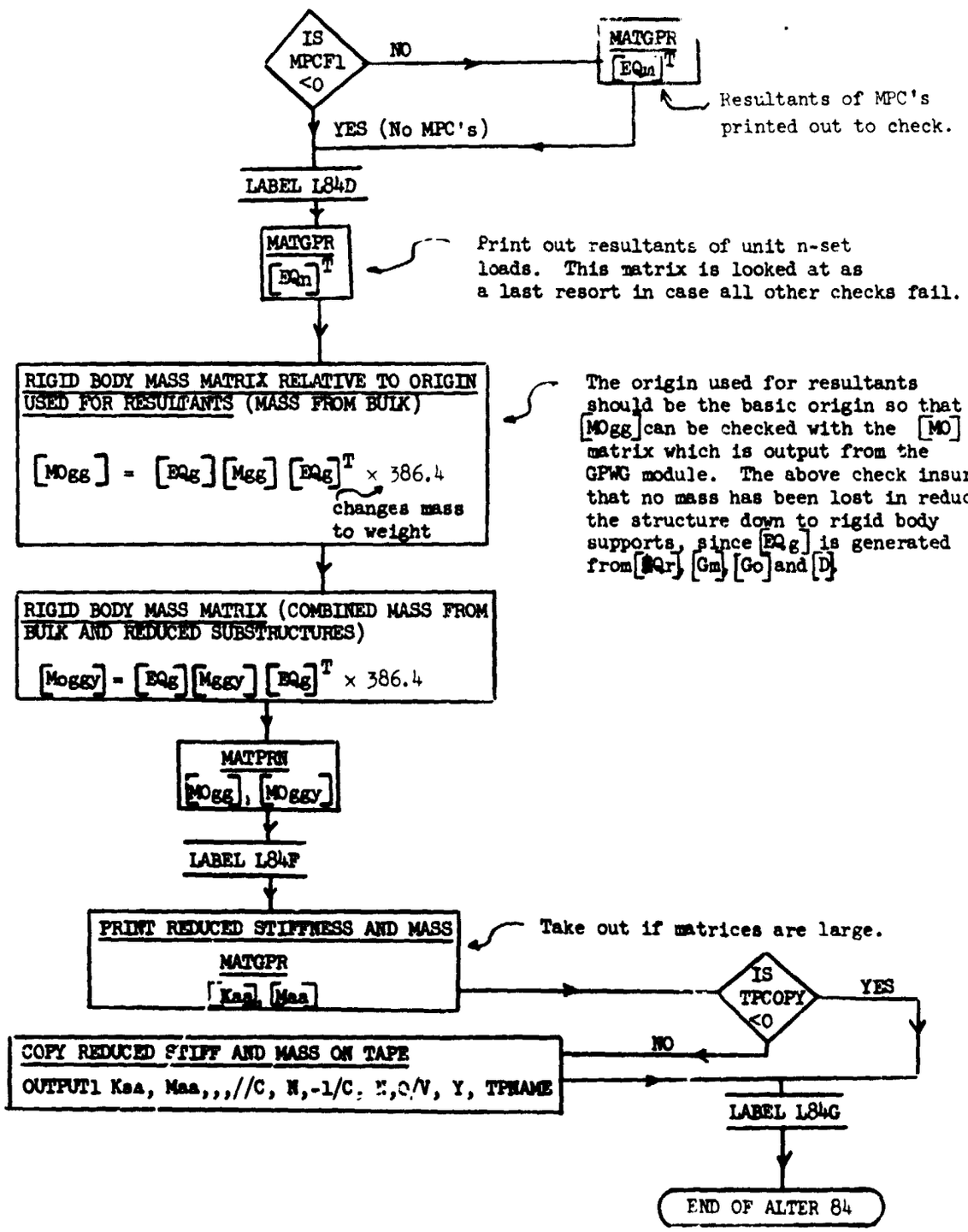
IS MPCF1 <0
NO
MATGPR [EQn]T
Resultants of MPC's printed out to check.
YES (No MPC's)
LABEL L84D
MATGPR [EQn]T
Print out resultants of unit n-set loads. This matrix is looked at as a last resort in case all other checks fail.
RIGID BODY MASS MATRIX RELATIVE TO ORIGIN USED FOR RESULTANTS (MASS FROM BULK)
[MOgg] = [EQg][Mgg][EQg]T × 386.4
changes mass to weight
The origin used for resultants should be the basic origin so that [MOgg] can be checked with the [MO] matrix which is output from the GPWG module. The above check insures that no mass has been lost in reducing the structure down to rigid body supports, since [EQg] is generated from [EQr], [Gm], [Go] and [D].
RIGID BODY MASS MATRIX (COMBINED MASS FROM BULK AND REDUCED SUBSTRUCTURES)
[Moggv] = [EQg][Mggv][EQg]T × 386.4
MATPRN [MOgg], [MOggv]
LABEL L84F
PRINT REDUCED STIFFNESS AND MASS
MATGPR [Kaa], [Maa]
Take out if matrices are large.
IS TPCOPY <0
YES
NO
COPY REDUCED STIFF AND MASS ON TAPE
OUTPUT1 Kaa, Maa,,,//C, N,-1/C, N,0/V, Y, TPNAME
LABEL L84G
END OF ALTER 84

ALTER 89,89 DETAILED FLOW

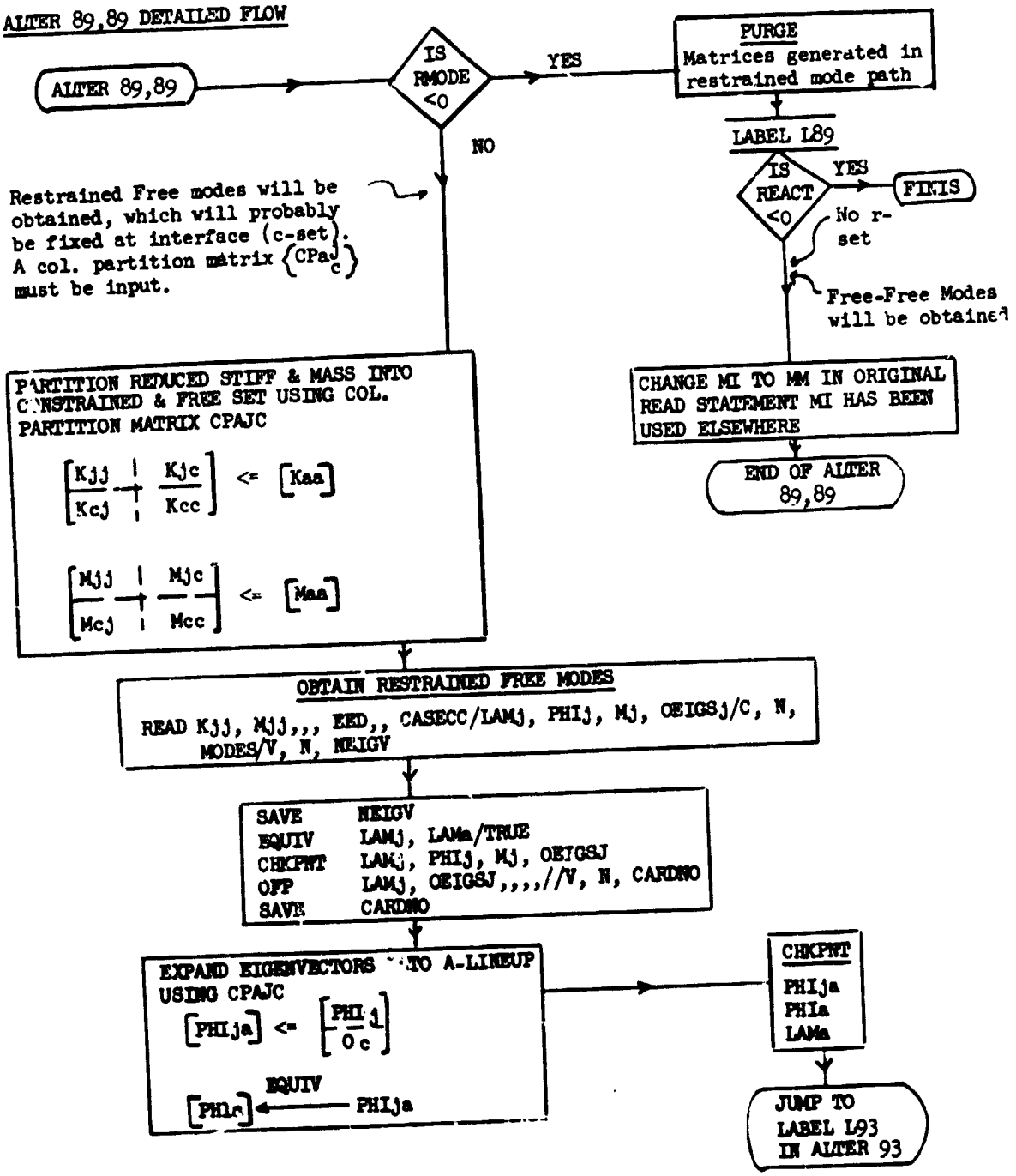

ALTER 112 DETAILED FLOW

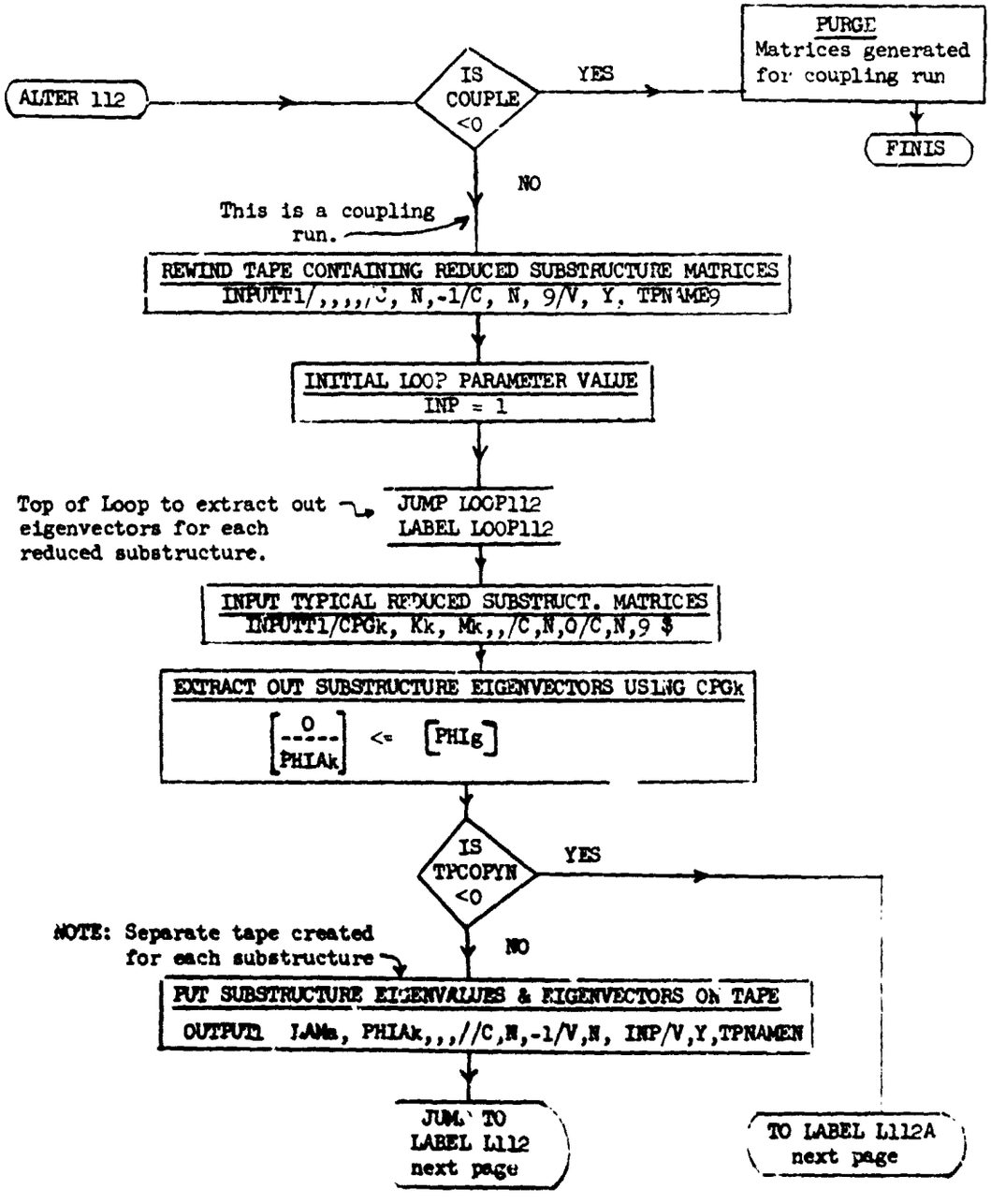

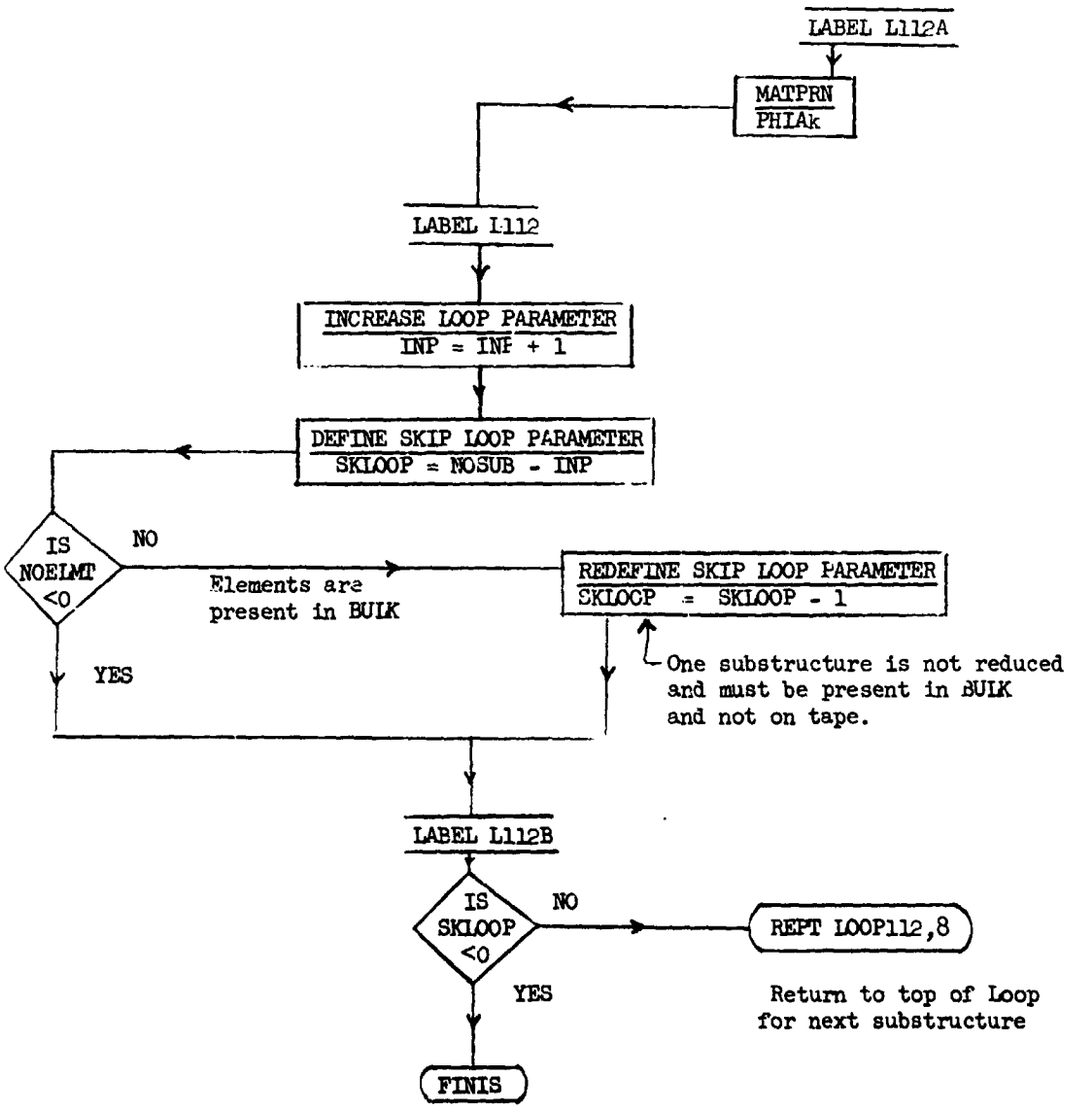
LABEL L112A
MATPRN
PHIAk
LABEL L112
INCREASE LOOP PARAMETER
INP = INP + 1
DEFINE SKIP LOOP PARAMETER
SKLOOP = NOSUB - INP
IS
NOELMT
<0
NO
Elements are
present in BULK
REDEFINE SKIP LOOP PARAMETER
SKLOOP = SKLOOP - 1
One substructure is not reduced
and must be present in BULK
and not on tape.
YES
LABEL L112B
IS
SKLOOP
<0
NO
REPT LOOP112,8
Return to top of Loop
for next substructure
YES
FINIS

N A S T R A N E X E C U T I V E C O N T R O L D E C K E C H O

```
ID PHASE2,DPNTSR1
APP        DISP
TIME       30
CHKPNT   YES
SOL          3,0
DIAG     7,8,13,14,19,21,22
ALTER 2  $ PARAMETER DEFAULTS
PARAM    //C,N,NOP/V,Y,NOSUB=1
PARAM    //C,N,NOP/V,Y,TPCOPY=-1
PARAM    //C,N,NOP/V,Y,TPCOPYN=-1
PARAM    //C,N,NOP/V,Y,PMODE=-1
PARAM    //C,N,NOP/V,N,TRUE=-1
$
ALTER 24,23 $ DETERMINES COUPLING PARAMETER & PERFORMS PURGES
PARAM    //C,N,SUB/V,N,COUPLE/V,Y,NOSUB/C,N,2 $
PARAM    //C,N,AND/V,N,NOELMT/V,N,NOGENL/V,N,NOSIMP $
PARAM    //C,N,AND/V,N,NOINP/V,N,NOELMT/V,N,COUPLE $
COND     ER23,NOINP $ WILL EXIT IF NOT A COUPLING RUN & NO ELEMENTS
PURGE    GPST,KGGX/NOSIMP
CHKPNT   GPST,KGGX
COND     L23,COUPLE
PURGE    DGPST/TRUE
JUMP     L24
LABEL    ER23
PRTPARM  //C,N,0/C,N,NOINP $
EXIT
LABEL    L23
$
ALTER 24
LABEL    L24
ALTER 25
COND     L27,NOSIMP
ALTER 27
LABEL    L27
ALTER 29
COND     L29,COUPLE
JUMP     L30
LABEL    L29
ALTER 30
LABEL    L30
$
ALTER 37,37 $ IF COUPLING RUN,COMBINES SUBSTRUCTURES.
$            THE FOLLOWING MATRICES FOR EACH SUBSTRUCT. ASSUMED ON INPT
$            CPGI = COLUMN PARTITIONG VECTOR FOR MERGING KI & MI
$            KI & MI = REDUCED STIFFNESS & MASS
PURGE    CPGI,KI,MI,KGGI,MGGI,KGGS,MGGS,KGT,MGT/COUPLE
COND     L370,COUPLE  $ SKIP,NOT A COUPLING RUN
INPUTT1  /,,,,/C,N,-3/C,N,9/V,Y,TPNAME9 $ LIST TAPE & REWIND
PARAM    //C,N,NOP/V,N,PASS=1  $ INITIAL LOOP PASS PARAMETER
```

N A S T R A N E X E C U T I V E C O N T R O L D E C K E C H O

```
JUMP     LOOP37
LABEL    LOOP37  $ TOP OF LOOP
PARAM    //C,N,SUB/V,N,PASS1/V,N,PASS/C,N,2
INPUTT1  /CPGI,KI,MI,,/C,N,0/C,N,9 $
COND     L37,PASS1   $ SKIP TO L37 IF FIRST PASS
JUMP     L37A
LABEL    L37
MERGE,   ,,,KI,CPGI,/KGGS/C,N,-1/C,N,2/C,N,6
MERGE,   ,,,MI,CPGI,/MGGS/C,N,-1/C,N,2/C,N,6
LABEL    L37A
COND     L37B,PASS1   $ SKIP TO L37B IF FIRST PASS
MERGE,   ,,,KI,CPGI,/KGGI/C,N,-1/C,N,2/C,N,6
MERGE,   ,,,MI,CPGI,/MGGI/C,N,-1/C,N,2/C,N,6
ADD      KGGS,KGGI/KGT $
EQUIV    KGT,KGGS/TRUE
ADD      MGGS,MGGI/MGT $
EQUIV    MGT,MGGS/TRUE
LABEL    L37B
PARAM    //C,N,ADD/V,N,PASS/V,N,PASS/C,N,1
PARAM    //C,N,SUB/V,N,SKIP2/V,Y,NOSUB/V,N,PASS
COND     L37C,NOELMT
PARAM    //C,N,SUB/V,N,SKIP2/V,N,SKIP2/C,N,1
LABEL    L37C
COND     L37D,SKIP2
DEPT     LOOP37,4
LABEL    L37D
CHKPNT   KGGS,MGGS
ADD      KGGX,KGGS/KGGY $
ADD      MGG,MGGS/MGGY $
CHKPNT   KGGY,MGGY
EQUIV    KGGY,KGG/NOGENL $
$
ALTER  40,40
SMA3     GEI,KGGY/KGG/V,N,LUSET/V,N,NOGENL/V,N,NOSIMP
ALTER  48,48
ADD      MGG,/MGG/C,Y,ALPHA=(386.4,0.0) $
MATGPR   GPL,USET,SIL,MGG//C,N,G
EQUIV    KGG,KNN/MPCF1/MGGY,MNN/MPCF1
ALTER  49
COND       L49,COUPLE
JUMP     LOOP4
LABEL    L49
ALTER  58,58
MCE2     USET,GM,KGG,MGGY,,/KNN,MNN,, $
ALTER  74
SEEMAT KAA,MAA,,,//C,N,PRINT
$
ALTER  84
PURGE    CPARL,CPFDA,CPNSF,CPGMN,EQR,EQL,EQA,EQD,EQF,EQN,EQM,EQG/REACT
PURGE    EX,EXT,EMT,EQNT,EQGT,EQGTC,MQGG,MQGGY/REACT
```

N A S T R A N E X E C U T I V E C O N T R O L D E C K E C H O

```
COND     L84E,REACT  $ R-SET MUST BE DEFINED TO GENERATE EQG
PURGE    CPEQA/OMIT/CPNSE/SINGLE/CPGMN/MPCF1
VEC      USET/CPARL/C,N,A/C,N,E/C,N,L $
COND     LCP1,OMIT
VEC      USET/CPEQA/C,N,E/C,N,O/C,N,A $
LABEL    LCP1
COND     LCP2,SINGLE
VEC      USET/CPNSE/C,N,N/C,N,S/C,N,E $
LABEL    LCP2
COND     LCP3,MPCF1
VEC      USET/CPGMN/C,N,G/C,N,M/C,N,N $
LABEL    LCP3
CHKPNT   CPEQA,CPNSE,CPGMN,CPARL
PURGE    EQD/OMIT/EQM/MPCF1
TRNSP    DM/DMT
MPYAD    EQR,DMT,/EQL/C,N,0/C,N,1/C,N,0
MERGE    EQR,,EQL,,CPARL,/EQA/C,N,1/C,N,2/C,N,2
EQUIV    EQA,EQE/OMIT
COND     L84A,OMIT
TRNSP    GO/GOT
MPYAD    EQA,GOT,/EQD/C,N,0/C,N,1/C,N,0
MERGE    EQD,,EQA,,CPEQA,/EQE/C,N,1/C,N,2/C,N,2
LABEL    L84A
EQUIV    EQE,EQN/SINGLE
COND     L84B,SINGLE
MERGE,   ,,EQE,,CPNSE,/EQN/C,N,1/C,N,2/C,N,2
LABEL    L84B
EQUIV    EQN,EQG/MPCF1
COND     L84C,MPCF1
TRNSP    GM/GMT
MPYAD    EQN,GMT,/EQM/C,N,0/C,N,1/C,N,0
MERGE    EQM,,EQN,,CPGMN,/EQG/C,N,1/C,N,2/C,N,2
LABEL    L84C
CHKPNT   EQL,EQA,EQD,EQE,EQN,EQM,EQG
TRNSP    EQR/EQRT
MATGPR   GPL,USET,SIL,EQRT//C,N,R
MPYAD    KLR,DM,KDR/K/C,N,1 $
MATGPR   GPL,USET,SIL,X//C,N,R
MPYAD    EQR,X,/EX/C,N,0/C,N,1/C,N,0 $
TRNSP    EX/EXT
MATGPR   GPL,USET,SIL,EXT//C,N,R
COND     L84D,MPCF1
TRNSP    EQM/EQMT
MATGPR   GPL,USET,SIL,EQMT//C,N,M
LABEL    L84D
TRNSP    EQN/EQNT
MATGPR   GPL,USET,SIL,EQNT//C,N,N
TRNSP    EQG/EQGT
ADD      EQGT,/EQGTC/C,Y,ALPHA=(386.4,0.0) $
$  ASSUME CONVERSION OF MASS TO LBS = 386.4
```

N A S T R A N E X E C U T I V E C O N T R O L D E C K E C H O

```
SMPYAD    EIG,MGG,EIGTC,,,/MOGG/C,N,3/C,N,1/C,N,0 $
SMPYAD  EIG,MGGY,EIGTC,,,/MOGGY/C,N,3/C,N,1/C,N,0 $
MATPRN  MGG,MOGGY,,,// $
LABEL   L84E
COND    L84G,TPCOPY
OUTPUT1 KAA,MAA,,,//C,N,-1/C,N,0/V,Y,TPNAME
LABEL   L84G
ALTER 89,99
PURGE   KJJ,KCJ,KJC,KCC,MJJ,MCJ,MJC,MCC,PHIJ,MJ,OEIGSJ,PHIJA/RMODE
COND    L83,RMODE  $ IF - FREE-FREE MODES WILL BE OBTAINED
$ IF RESTRAINED MODES ARE TO BE OBTAINED CPAJC MUST INPUT
PARTN   KAA,CPAJC,/KJJ,KCJ,KJC,KCC/C,N,-1/C,N,2/C,N,6/C,N,2/C,N,2/C,N,6
PARTN   MAA,CPAJC,/MJJ,MCJ,MJC,MCC/C,N,-1/C,N,2/C,N,6/C,N,2/C,N,2/C,N,6
READ    KJJ,MJJ,,,EED,,CASECC/LAMJ,PHIJ,MJ,OEIGSJ/C,N,MODES/V,N,NEIGV $
SAVE    NEIGV
EQUIV    LAMJ,LAMA/TRUE
CHKPNT  LAMJ,PHIJ,MJ,OEIGSJ
DEF     LAMJ,OEIGSJ,,,,//V,N,CARDNO
SAVE    CARDNO
MERGE   PHIJ,,,,,CPAJC/PHIJA/C,N,1/C,N,2/C,N,2
EQUIV   PHIJA,PHIA/TRUE
CHKPNT  PHIJA,PHIA,LAMA
JUMP    L93
LABEL   L83
COND    FINIS,REACT
READ    KAA,MAA,MR,DM,EED,USET,CASECC/LAMA,PHIA,MM,OEIGS/C,N,MODES/V,N,
        NEIGV $
ALTER 91,91
CHKPNT  LAMA,PHIA,MM,OEIGS $
ALTER 93
LABEL   L93
$
ALTER 112
PURGE   CPGK,KK,MK,PHIAK/COUPLE
COND    FINIS,COUPLE
INPUTT1 /,,,,/C,N,-1/C,N,9/V,Y,TPNAME9  $ REWIND INP9
PARAM   //C,N,NIP/V,N,INP=1 $
JUMP    LOOP112
LABEL   LOOP112
INPUTT1 /CPGK,KK,MK,,/C,N,0/C,N,9 $
PARTN   PHIG,,CPGK/,PHIAK,,/C,N,1 $
COND    L112A,TPCOPYN
OUTPUT1 LAMA,PHIAK,,,  //C,N,-1/V,N,INP/V,Y,TPNAMEN
JUMP    L112
LABEL   L112A
MATPRN  PHIAK,,,,// $
LABEL   L112
PARAM   //C,N,ADD/V,N,INP/V,N,INP/C,N,1 $
PARAM   //C,N,SUB/V,N,SKLOOP/V,Y,NOSUB/V,N,INP
COND    L112B,NOELMT
```

N A S T R A N E X E C U T I V E C O N T R O L D E C K E C H O

```
PARAM    //C,N,SUB/V,N,SKLOOP/V,N,SKLOOP/C,N,1
LABEL    L1122
COND     FINIS,SKLOOP
REPT     LOOP112,8
ENDALTER
CEND
```

TABLE 1.- STATISTICAL DESCRIPTION OF 1/8-SCALE MODEL

COMPONENT	No. GRID POINTS	No. CBAR	No. CQDMEM2	No. CSHEAR	No. CROD	No. CTRMEM	No. CQUAD2	TOTAL No OF MEMBERS	SYMM. CASE		ANTI-SYMM. CASE	
									D.O.F. AFTER SPC & MPC	D.O.F. AFTER GUYAN	D.O.F. AFTER SPC & MPC	D.O.F. AFTER GUYAN
PAYLOAD	12	8	-	-	-	-	-	8	24	24	26	26
FIN	59	-	24	22	65	-	-	111	101	25	99	24
WING	192	-	149	81	187	8	-	425	531	183	531	183
DOORS	134	9	20	64	178	-	16	287	396	26	384	26
FUSELAGE	537	93	336	172	616	7	-	1224	1417	246	1368	222
TOTAL $\frac{1}{2}$ ORBITER	934	110	529	339	1046	15	16	2055	2469	504	2408	481
ORBITER ANALYSIS	215	CONTAINS 125 PLOTEL ELEMENTS							400	339	378	324

COMPONENT	No. GRID POINTS	No. FLUID POINTS	No. CBAR	No. CROD	No. CQUAD2	No. CTRIA2	No. CHEXA1	No. CFLUID	TOTAL No. OF MEMBERS	SYMM. CASE		ANTI-SYMM. CASE	
										D.O.F. AFTER SPC & MPC	D.O.F. AFTER GUYAN	D.O.F. AFTER SPC & MPC	D.O.F. AFTER GUYAN
S R B	755	-	99	-	268	-	432	-	799	3114	212	3114	212
LH_2 TANK	215	-	135	26	172	16	-	-	349	1107	216	1111	194
LOX TANK	137	51	8	-	112	16	-	50	186	766			
TOTAL $\frac{1}{2}$ BOOSTER	1107	51	242	26	552	32	432	50	1334	4987			

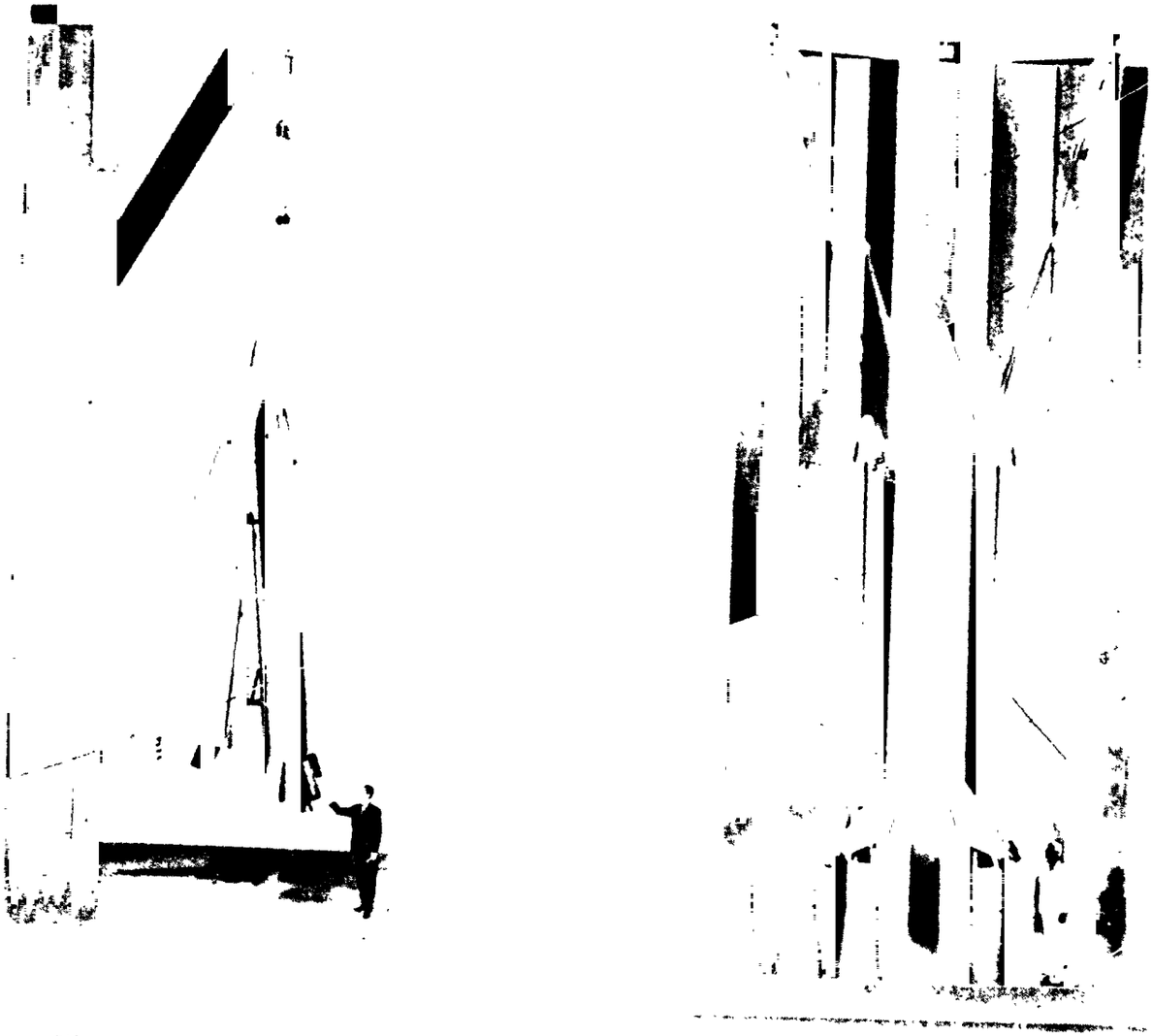

Figure 1.- Mock-up of 1/8-scale space shuttle structural dynamics model.

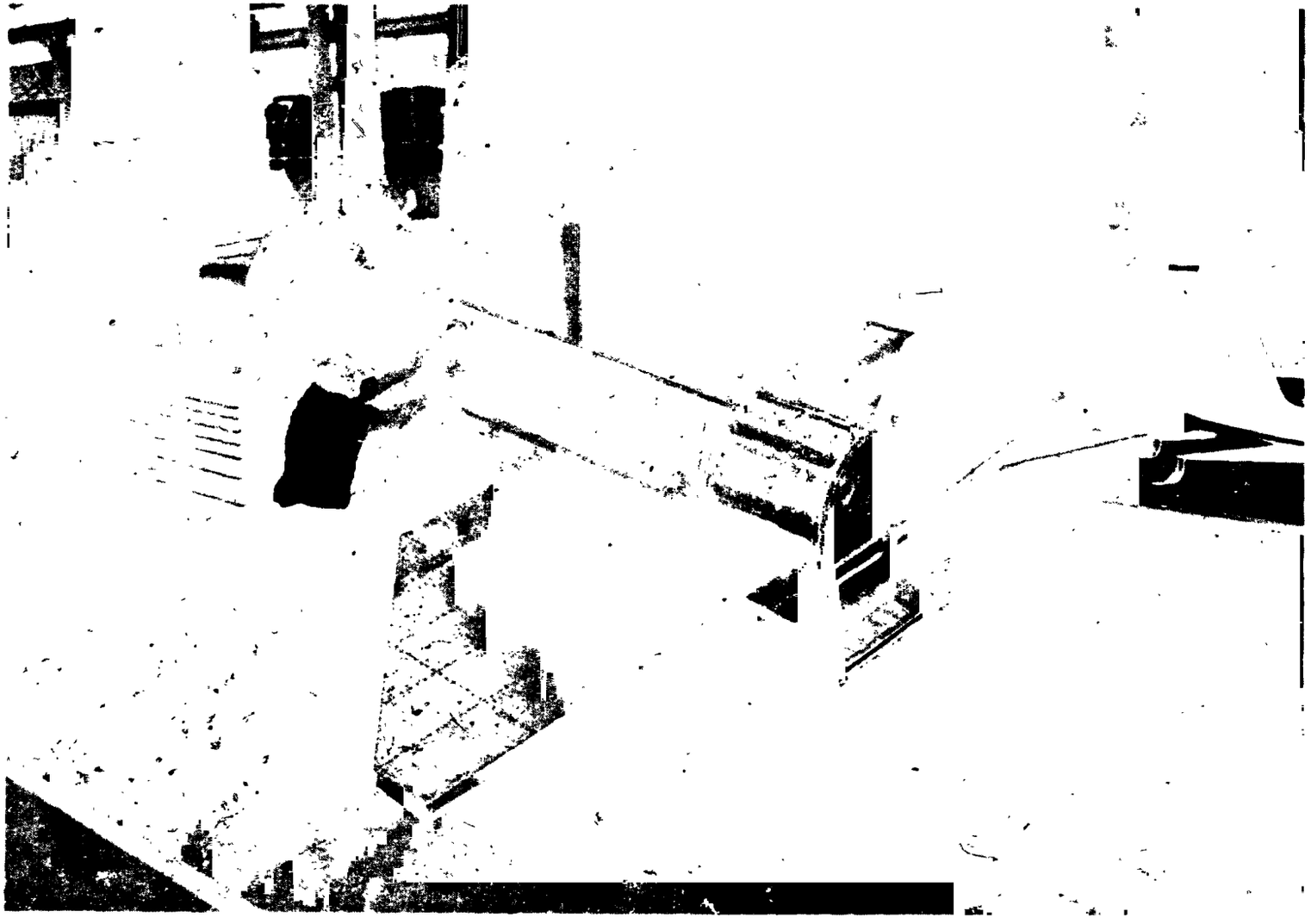

Figure 2.- The 1/8-scale orbiter model.

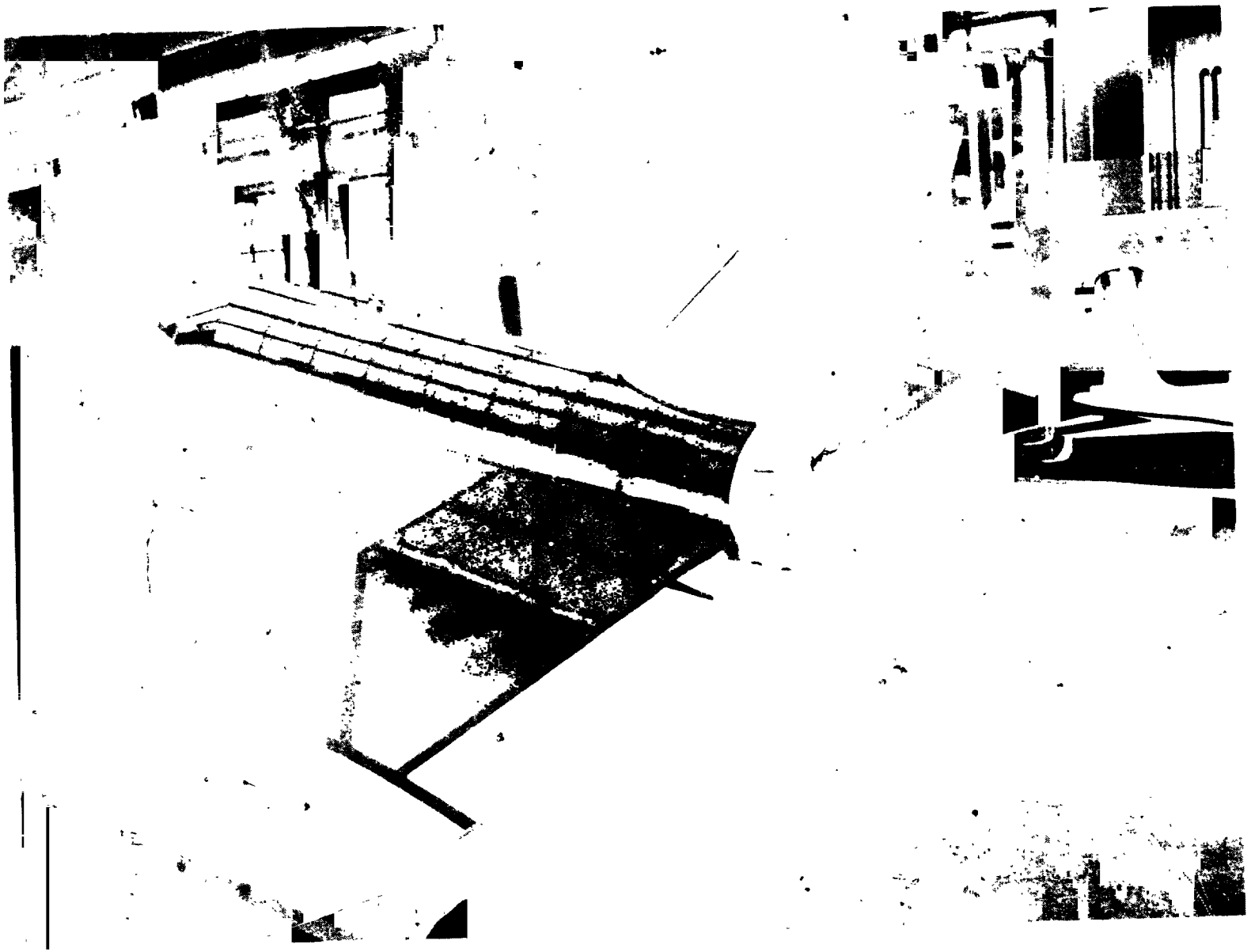

Figure 3.- Orbiter with plastic fairings.

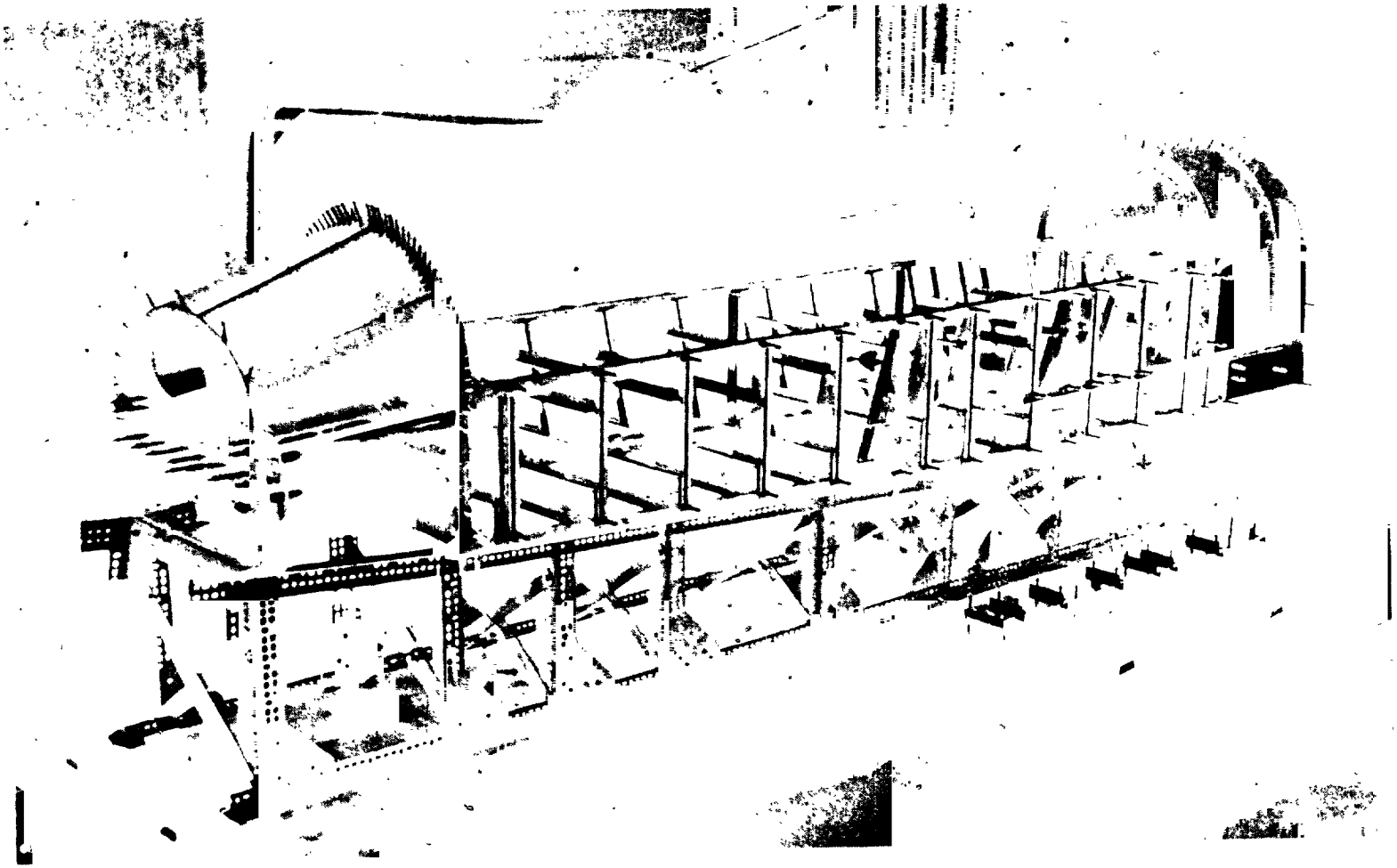

Figure 4.- Orbiter fuselage under assembly.

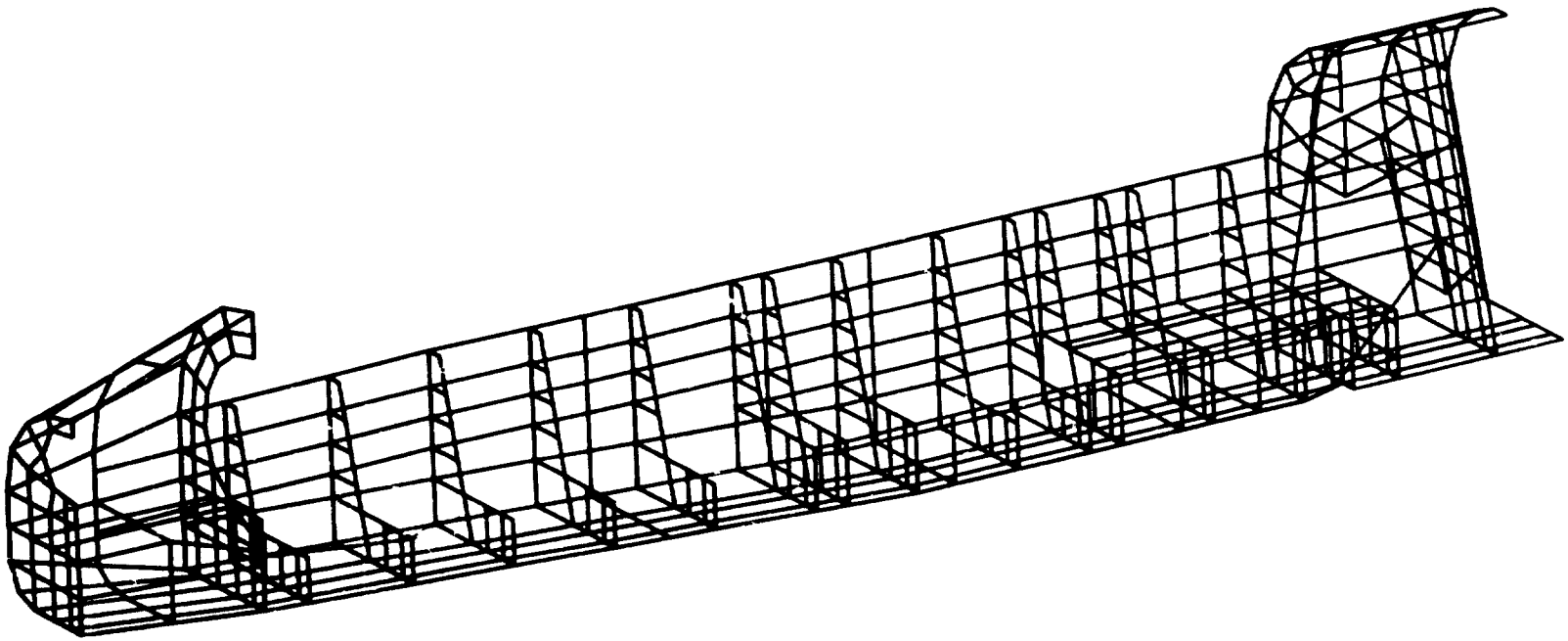

Figure 5.- NASTRAN plot of orbiter fuselage.

Figure 6.- Orbiter wing under assembly.

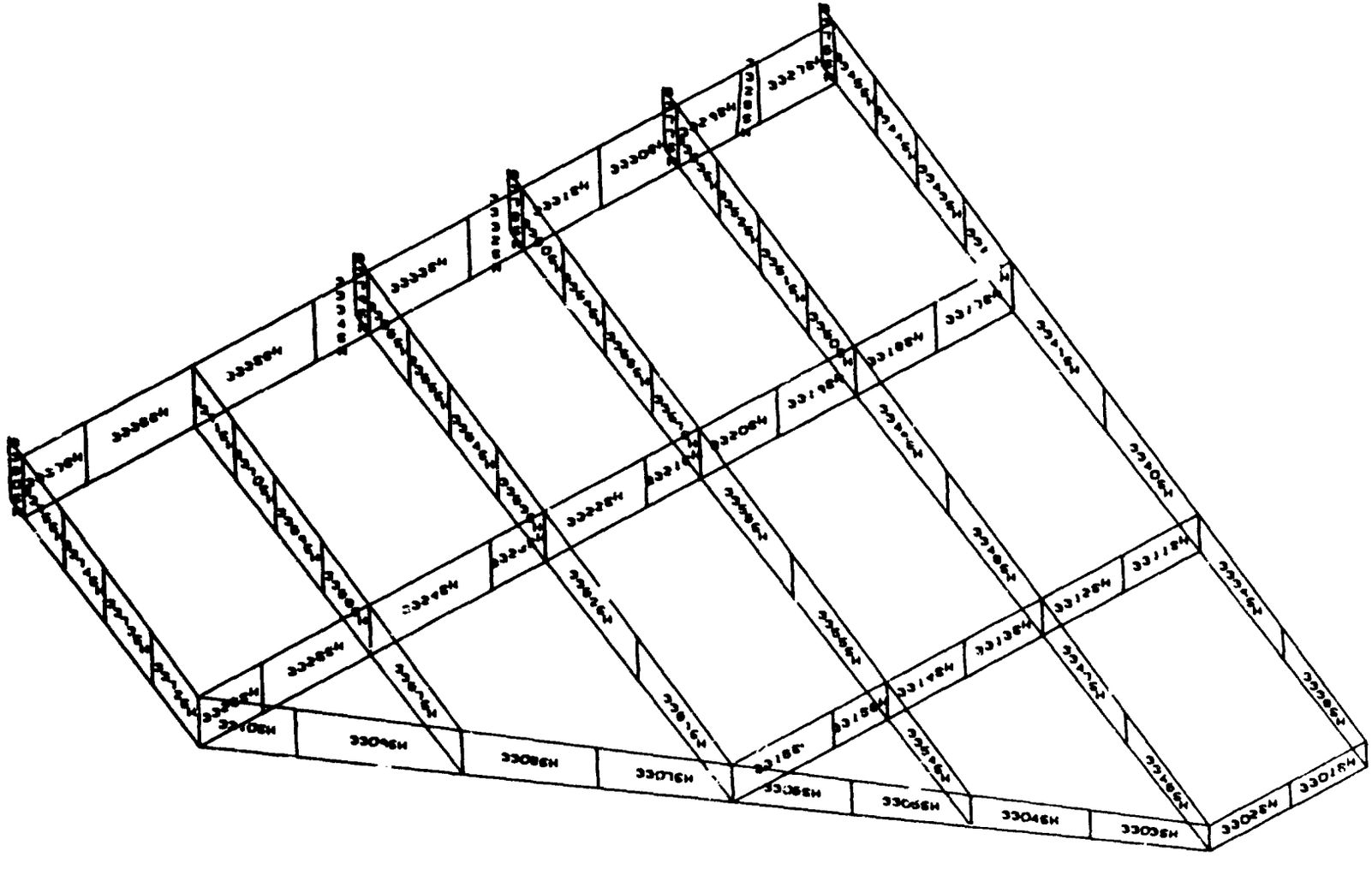

Figure 7.- NASTRAN plot of wing rib and spar shear webs.

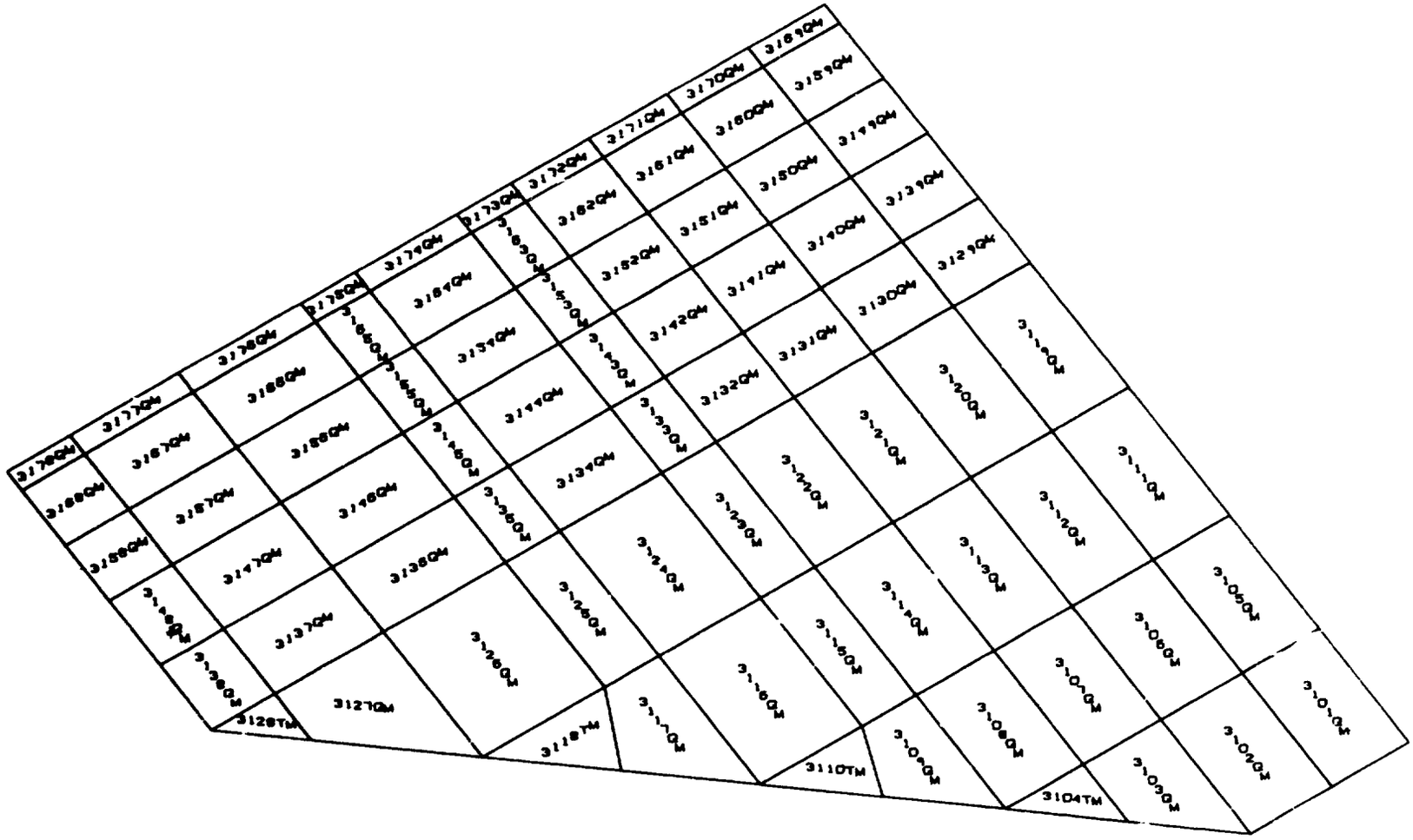

Figure 8.- NASTRAN plot of wing top cover.

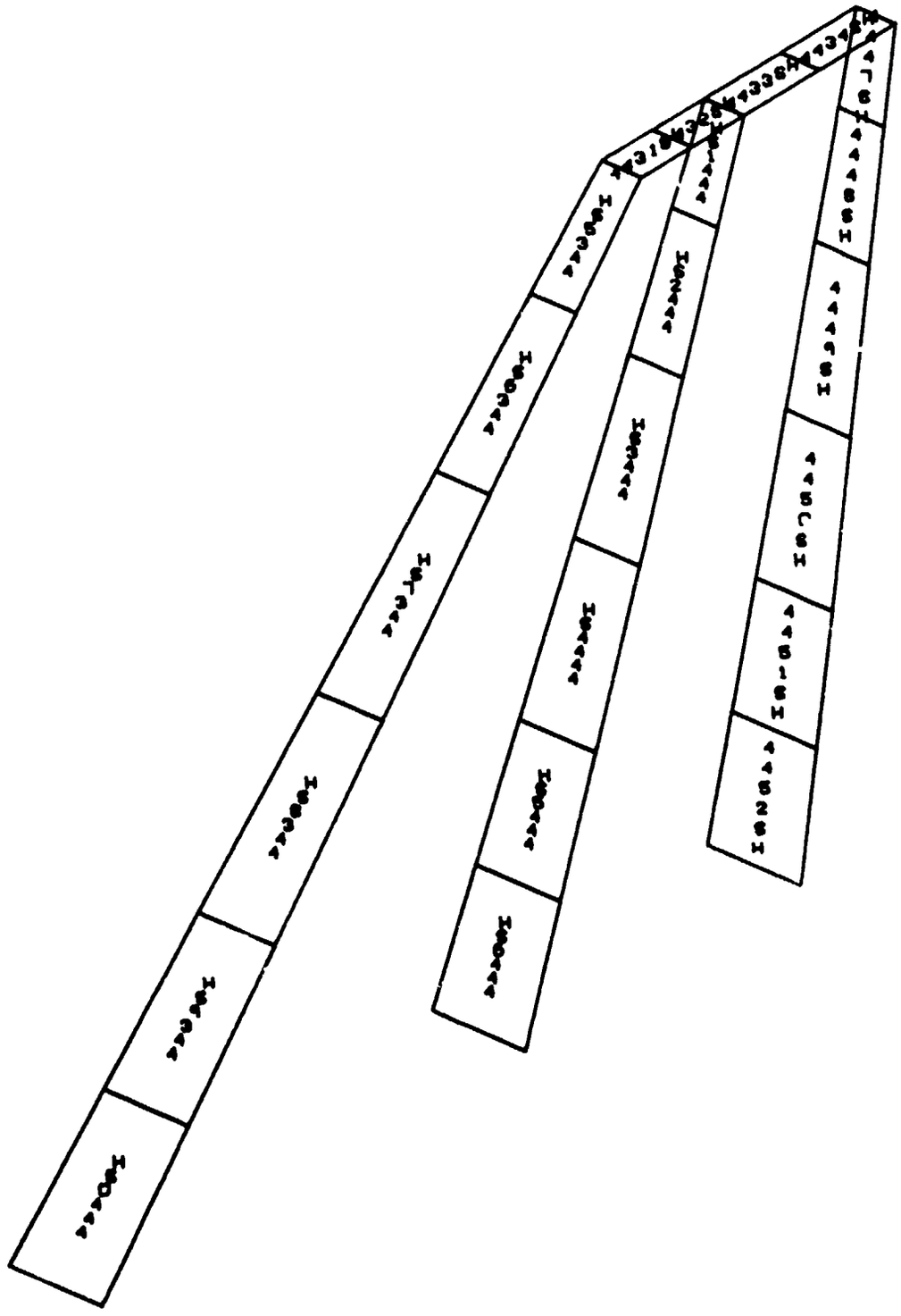

Figure 9.- NASTRAN plot of fin webs.

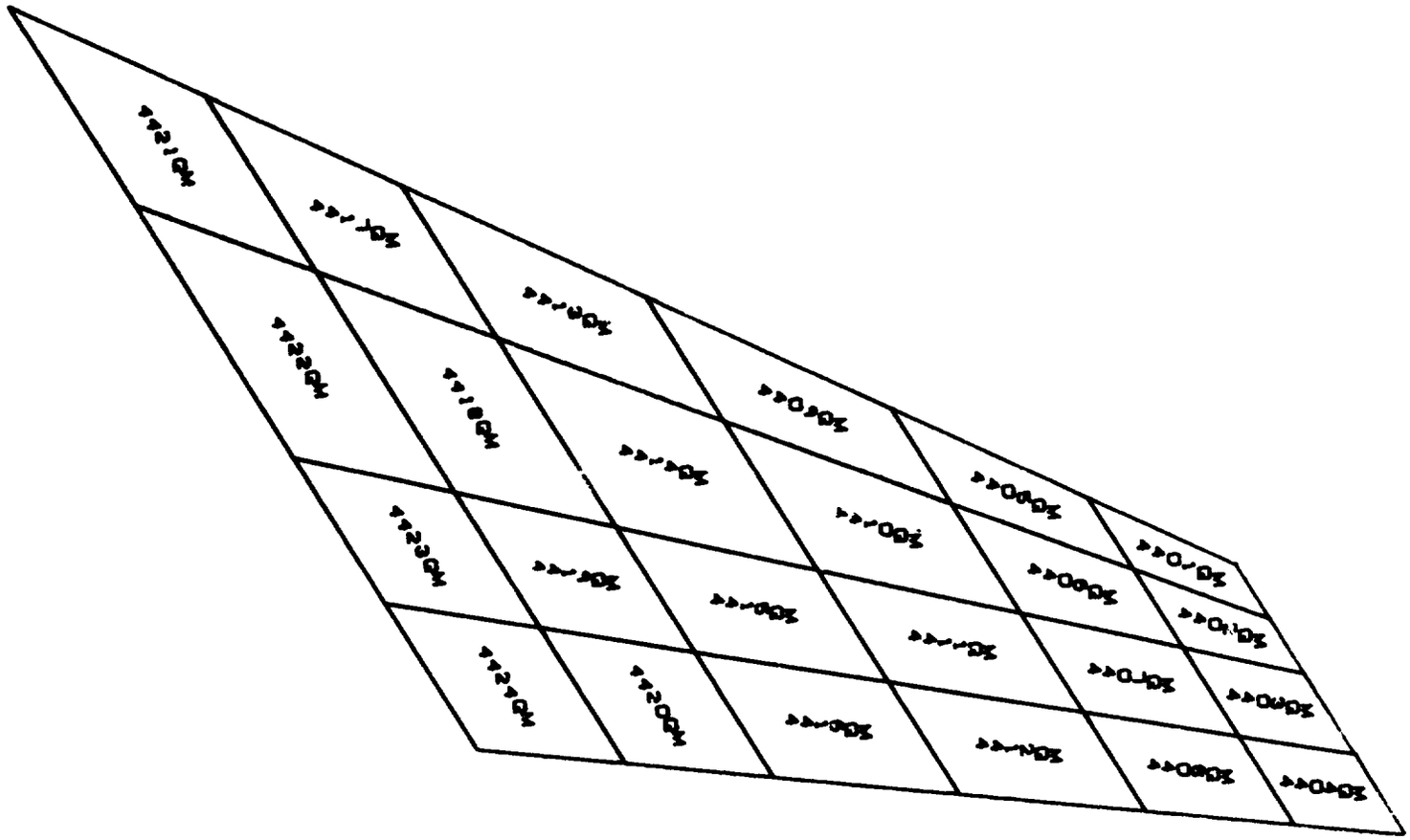

Figure 10.- NASTRAN plot of fin cover.

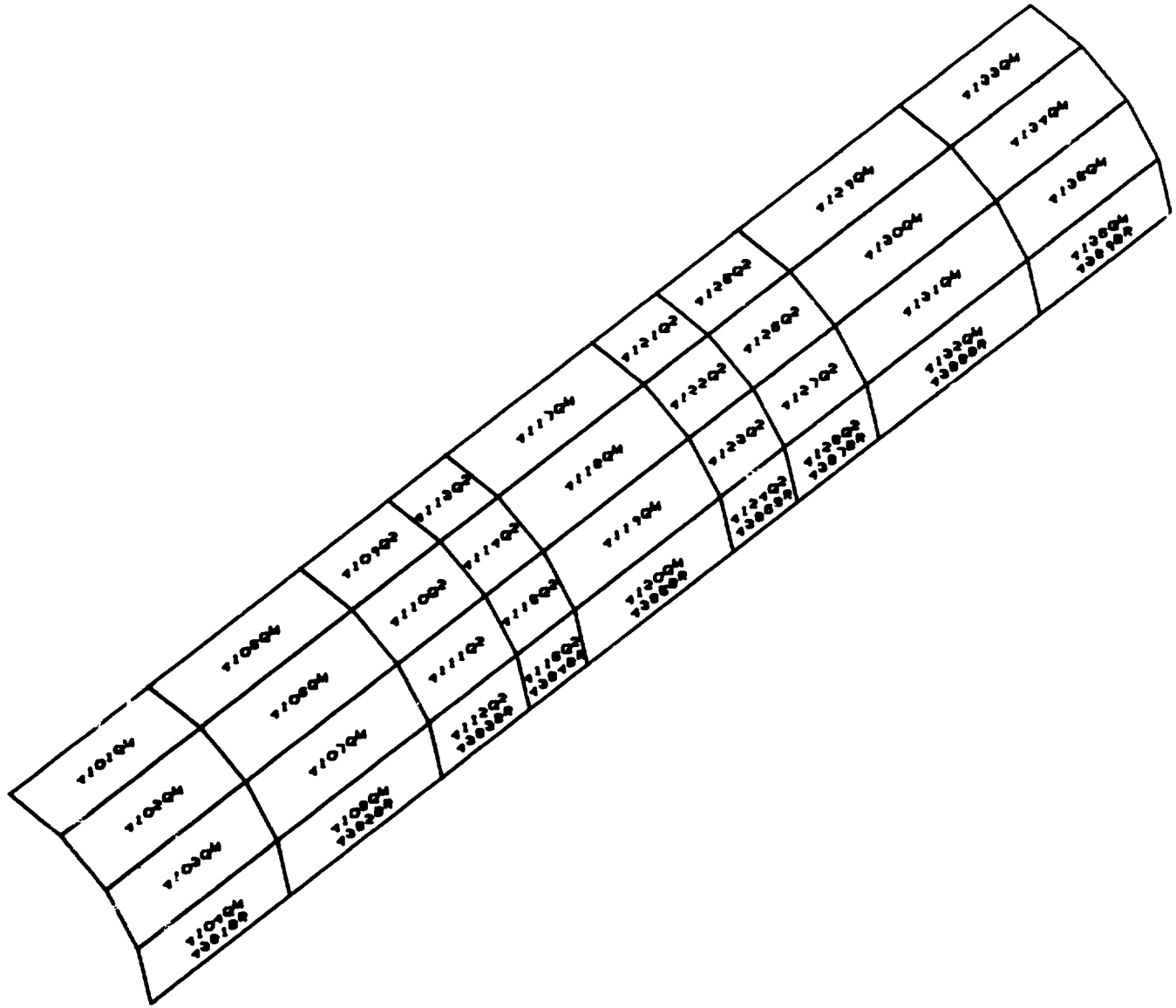

Figure 11.- NASTRAN plot of cargo bay door covers.

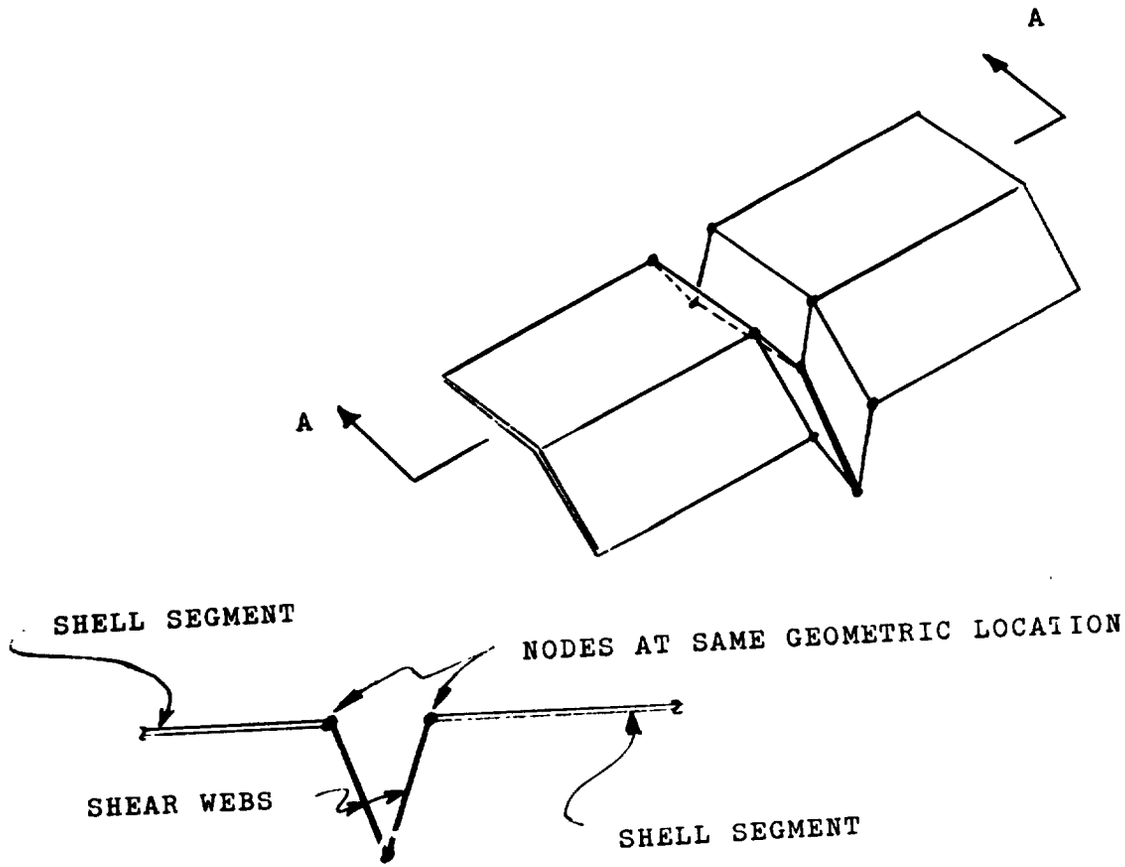

Figure 12.- Schematic of cargo door joints.

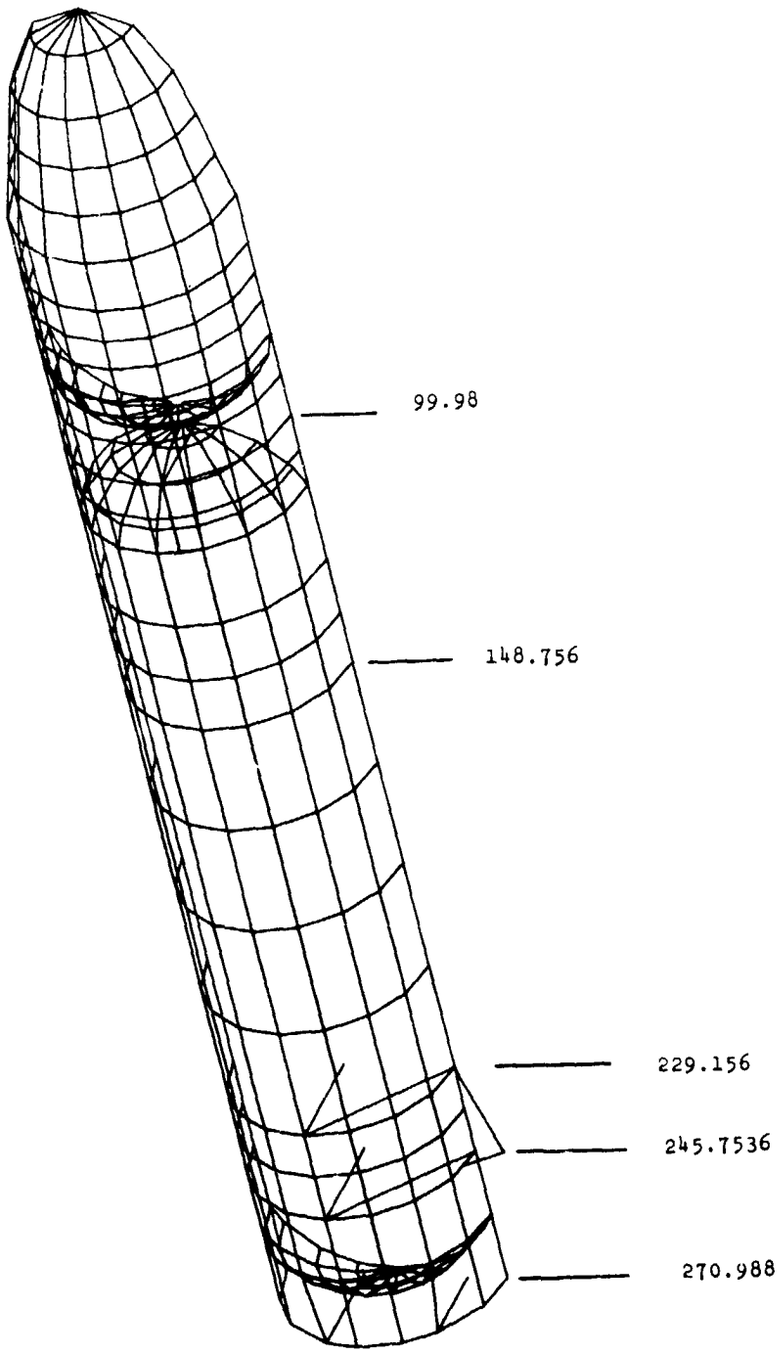

Figure 13.- NASTRAN plot of external tank.

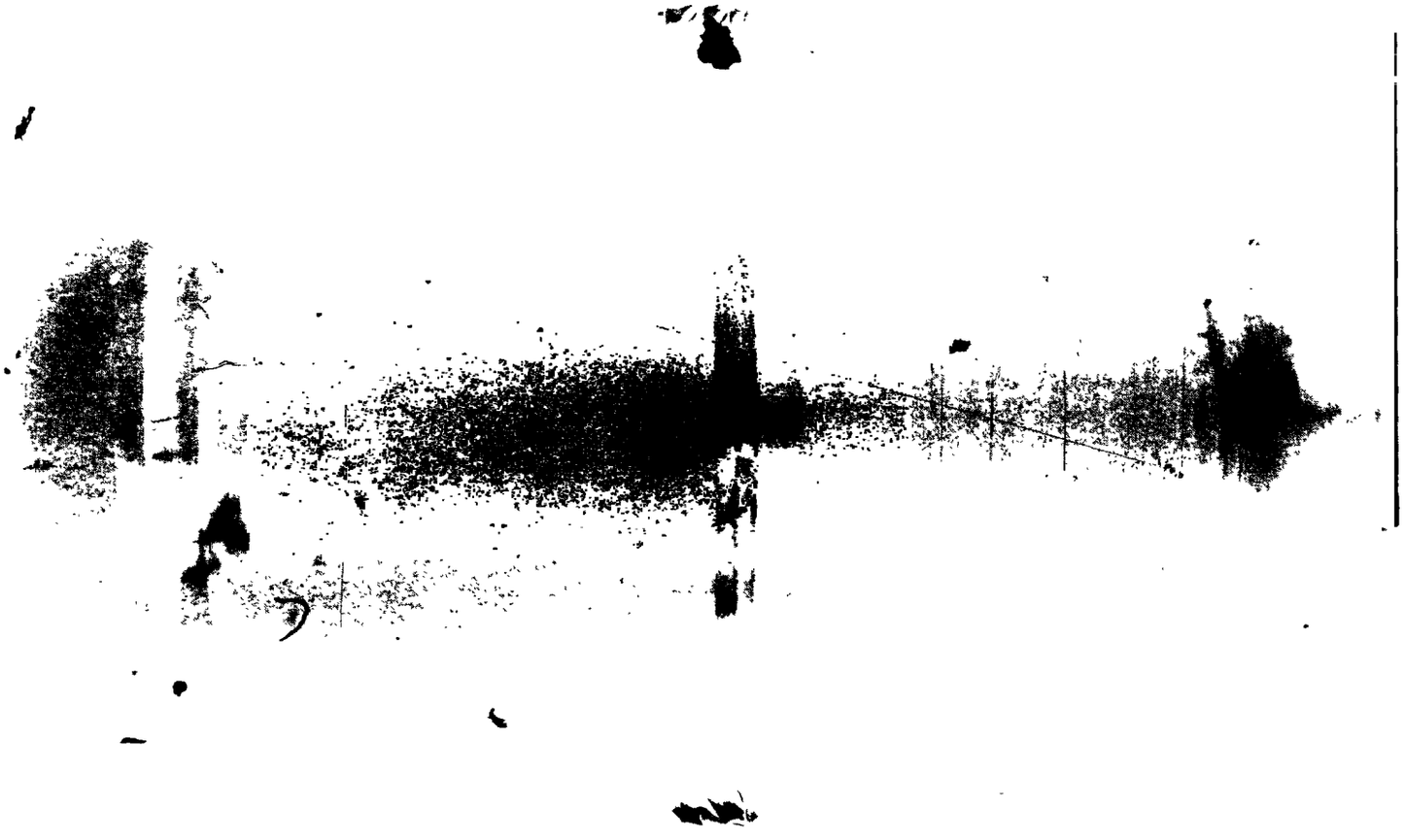

Figure 14.- Liquid oxygen tank.

Figure 15.- LOX tank connected to inter tank skirt and forward tank/SRB interstage.

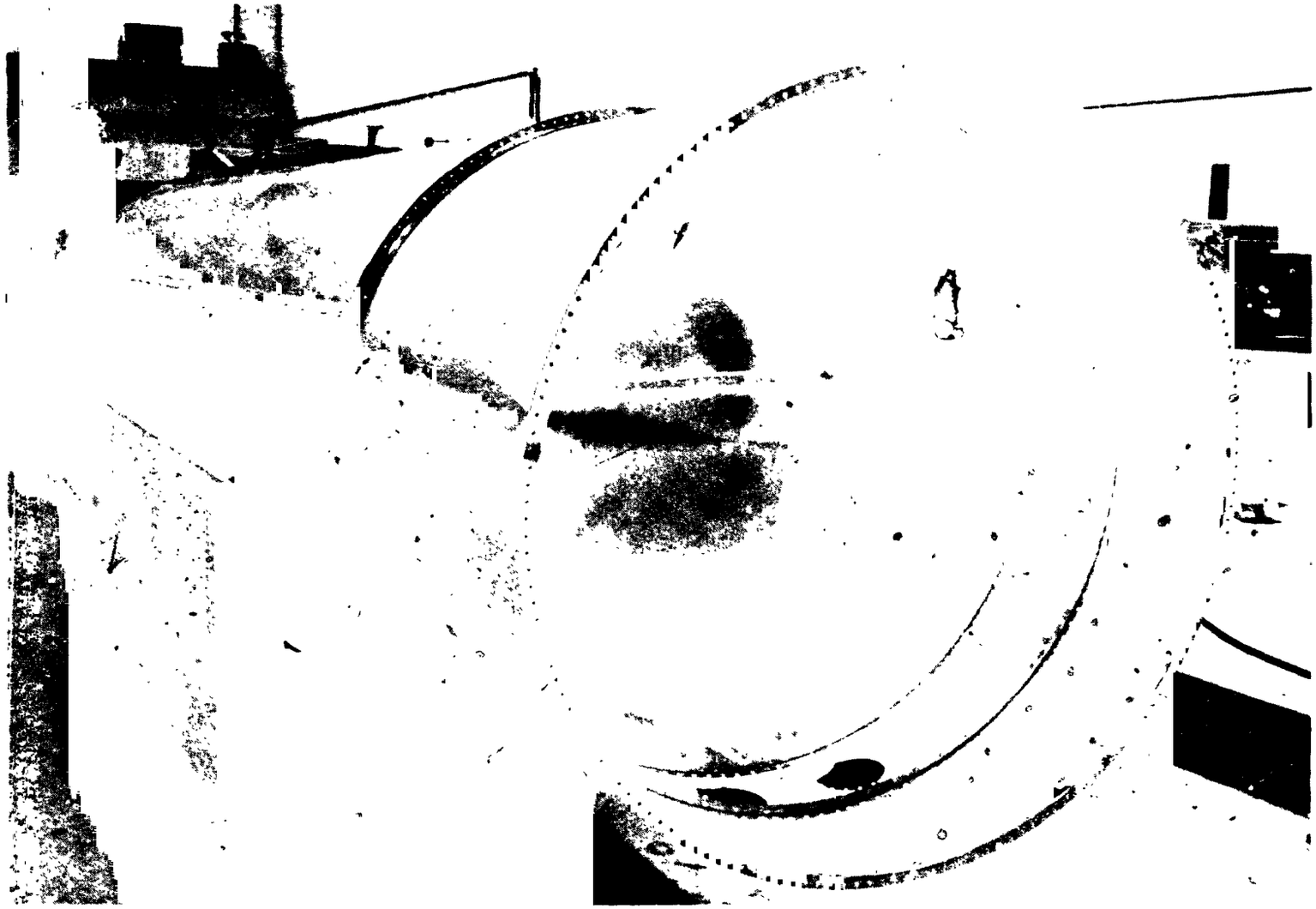

Figure 16.- LH_2 tank and inter tank skirt.

Figure 17.- Aft orbiter/tank interstage.

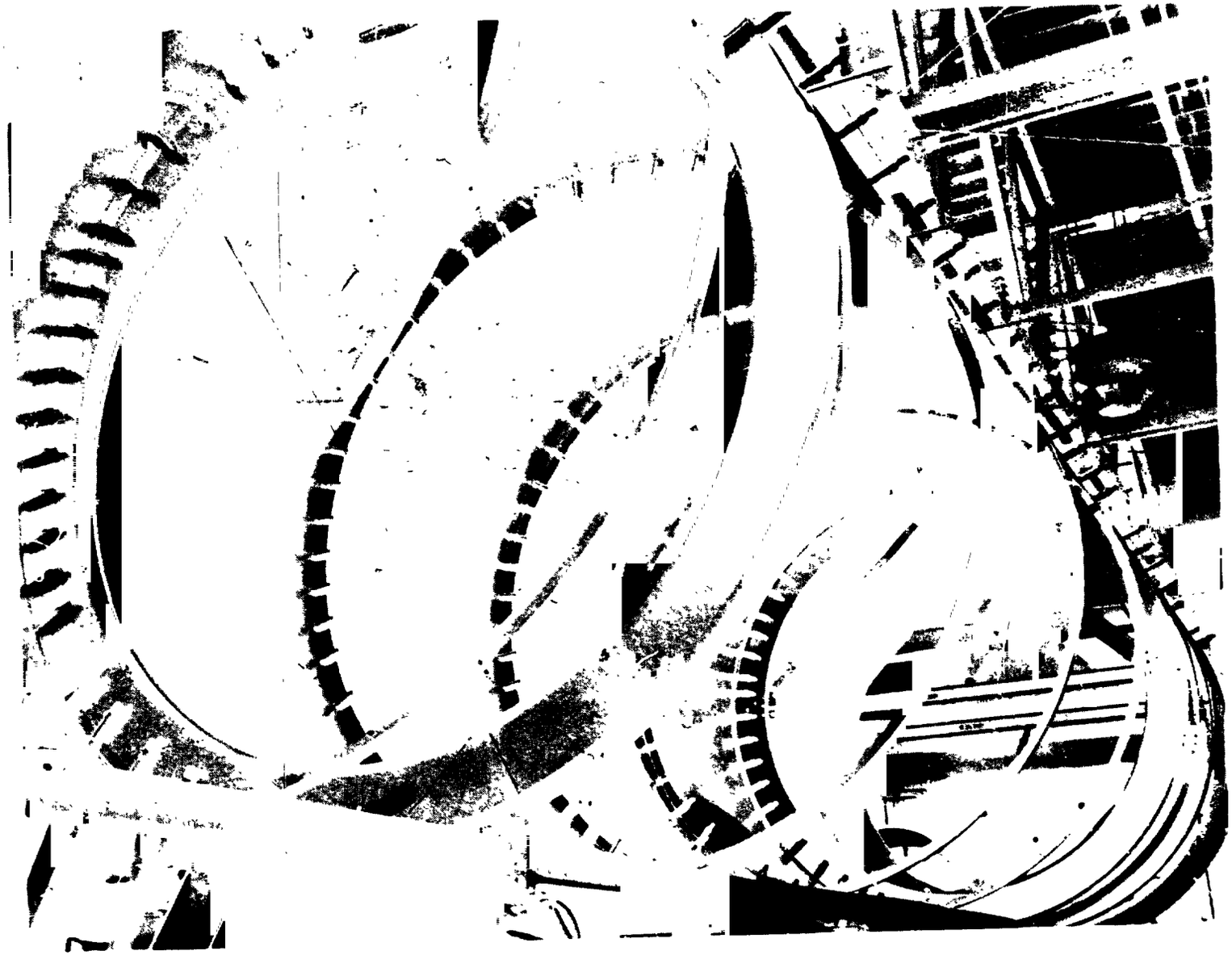

Figure 18.- LH_2 tank under assembly.

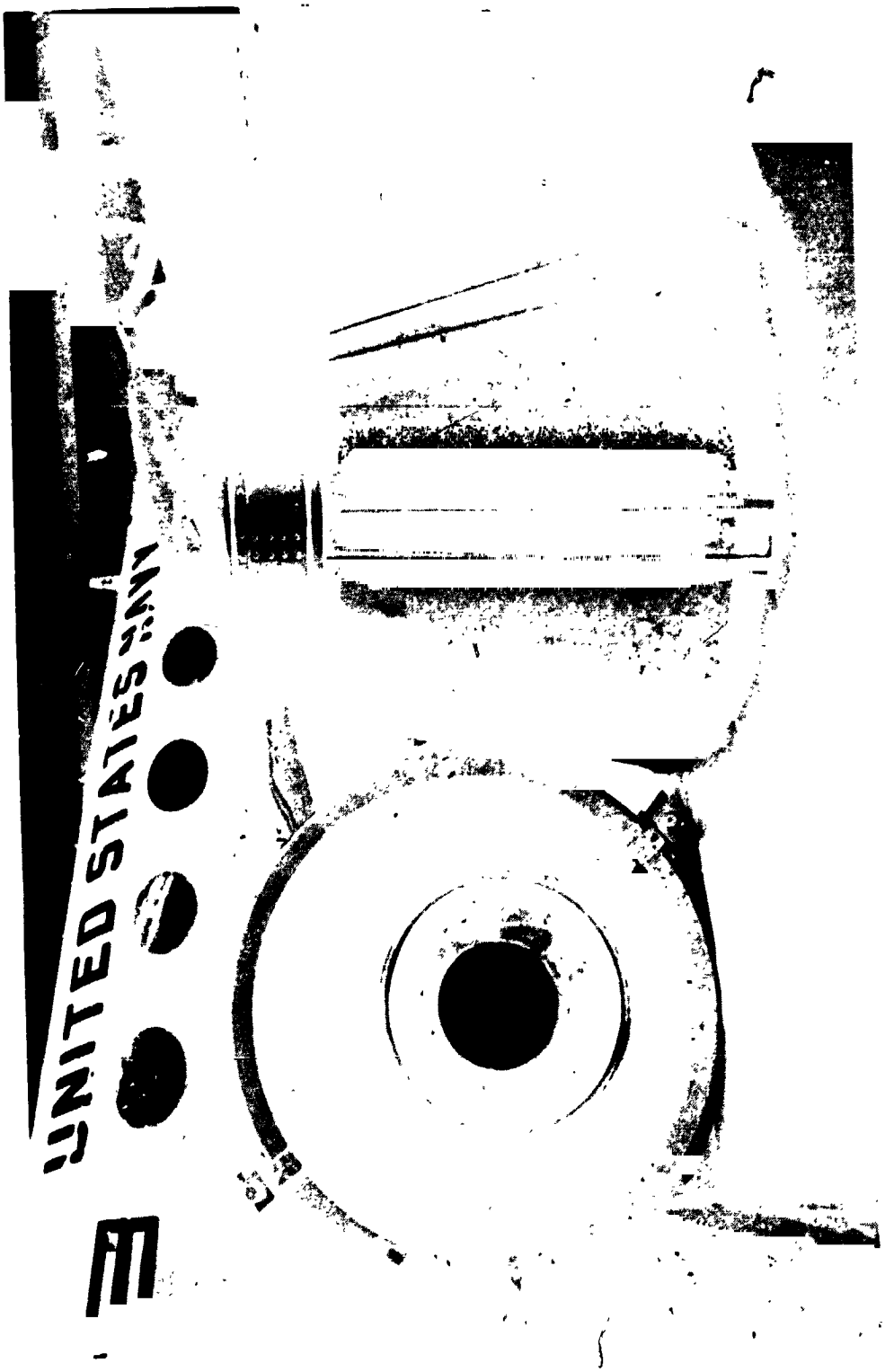

Figure 19.- Solid rocket booster aft skirt.

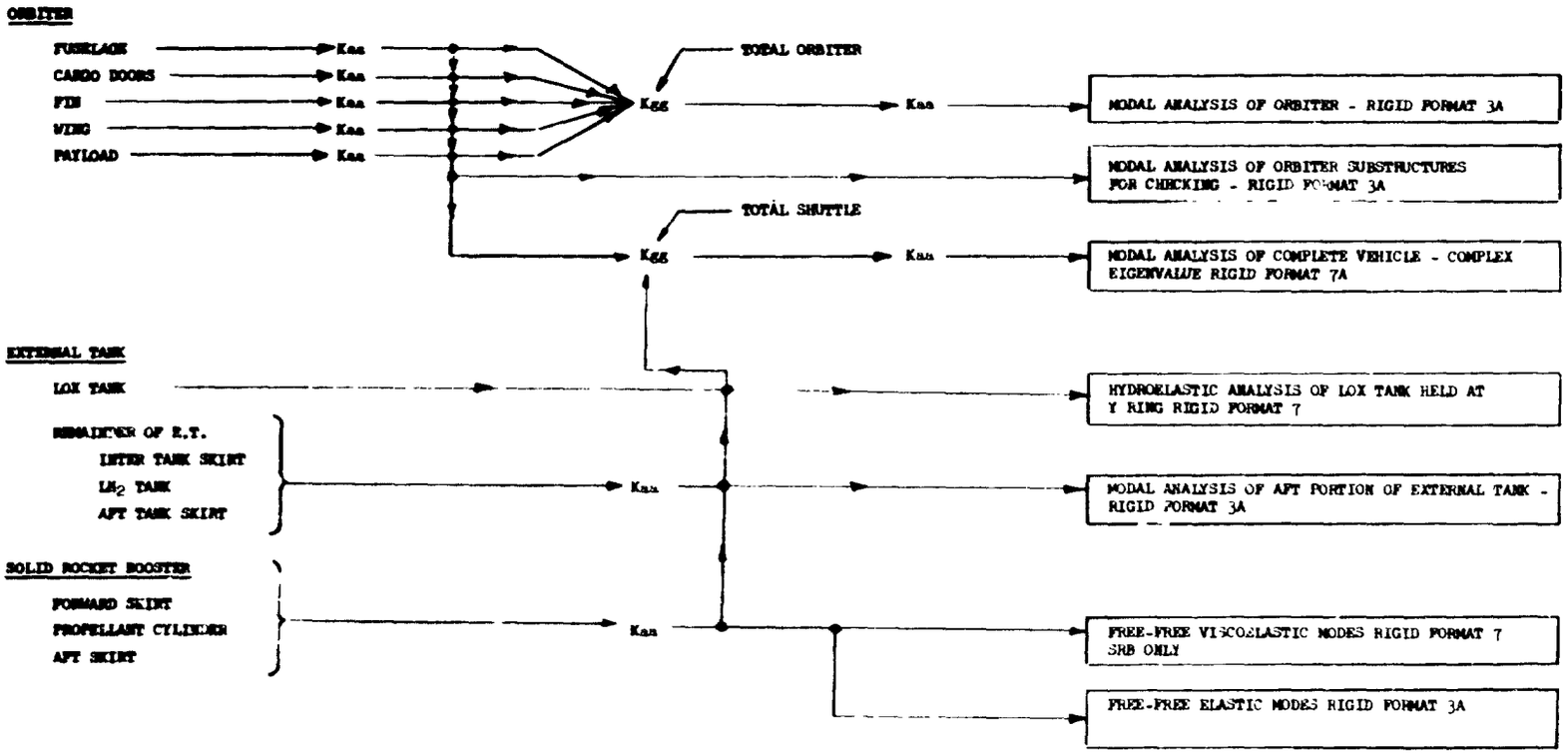

Figure 20.- Schematic diagram of analysis flow. The letter A affixed to the Rigid Format Number denotes DMAP Alteration of that format.

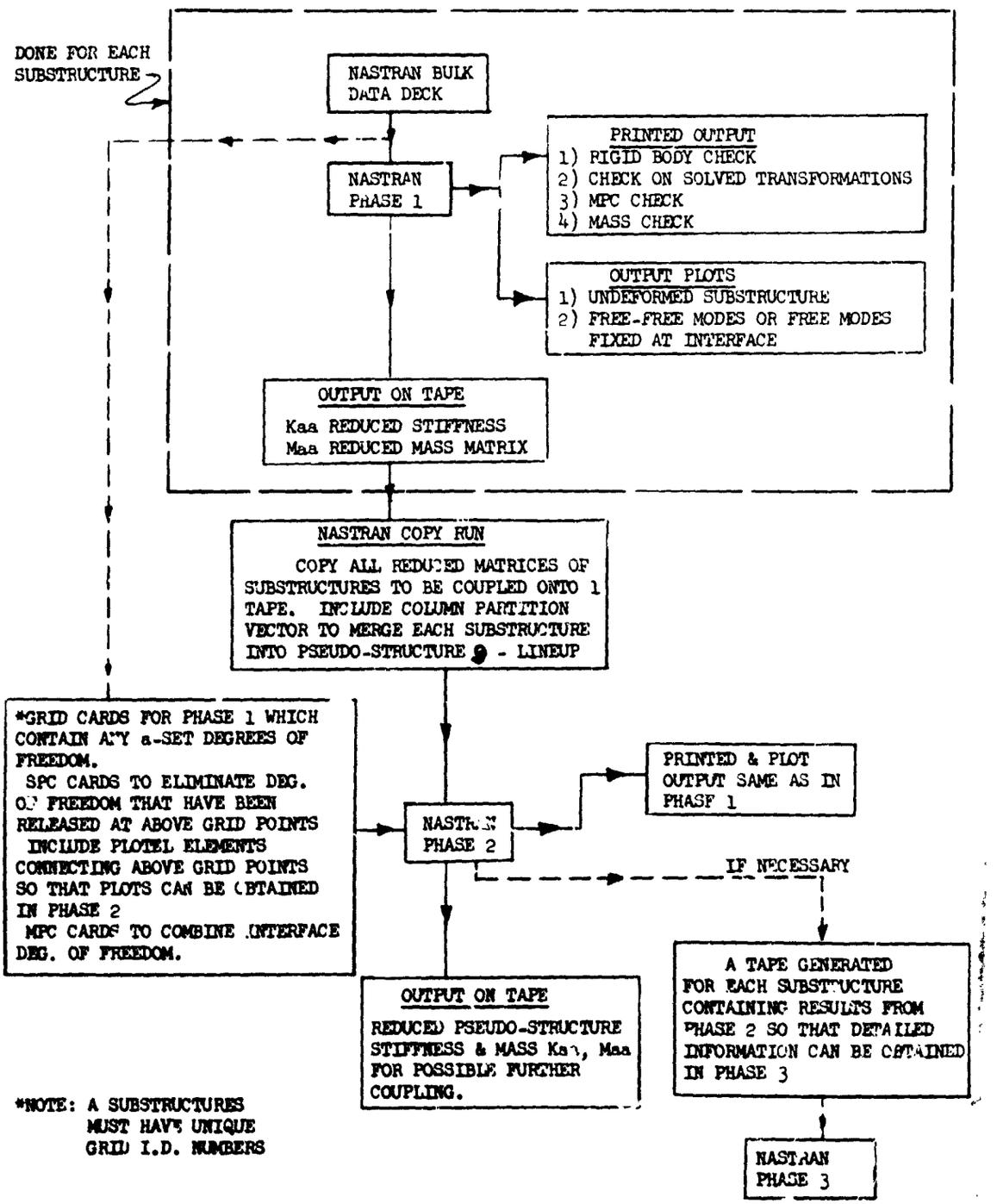

Figure 21.- Flow diagram for NASTRAN substructuring to obtain normal modes (Rigid Format 3).

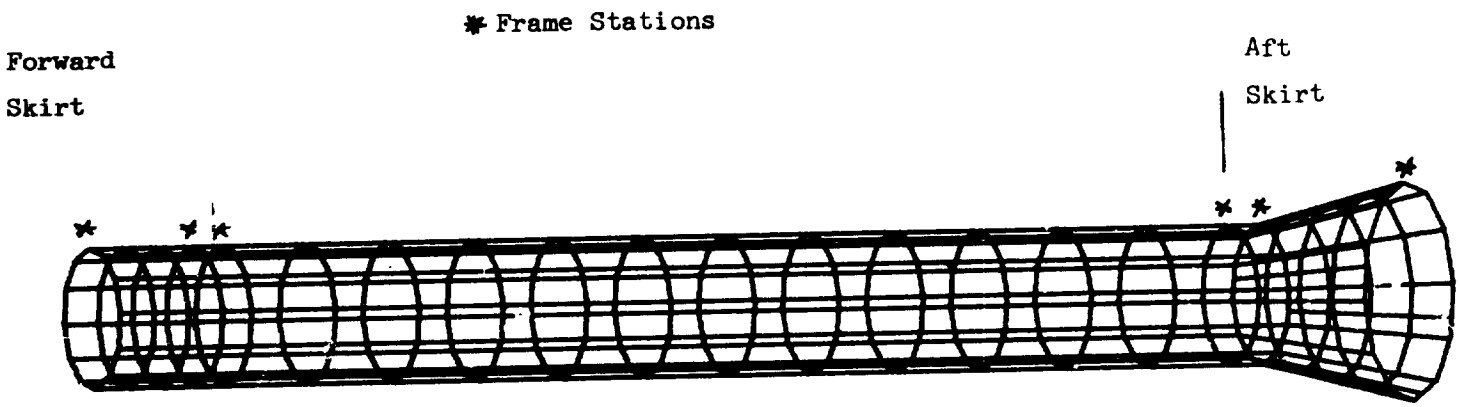

Figure 22.- Solid rocket booster idealization.

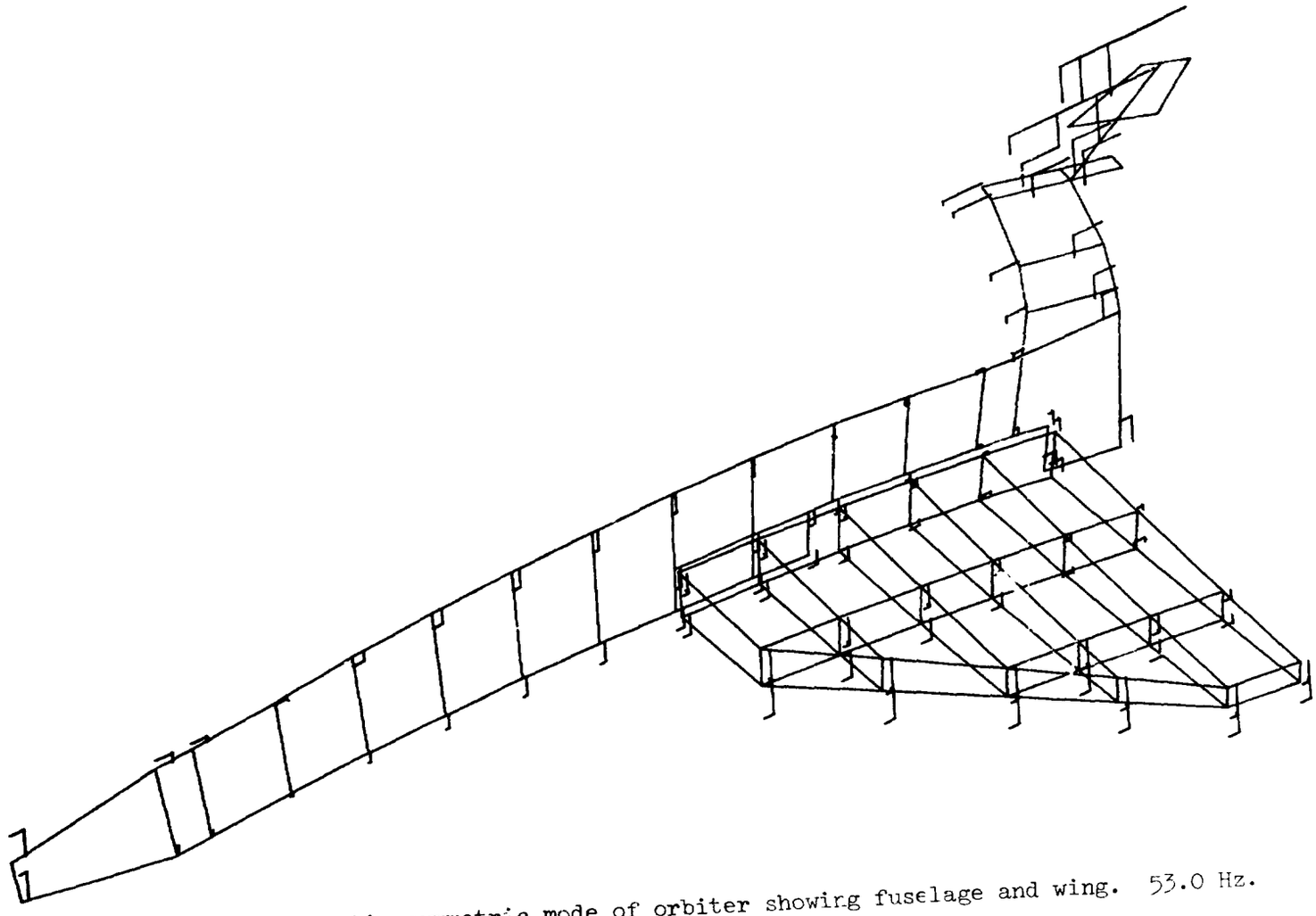

Figure 23.- First elastic symmetric mode of orbiter showing fuselage and wing. 53.0 Hz.

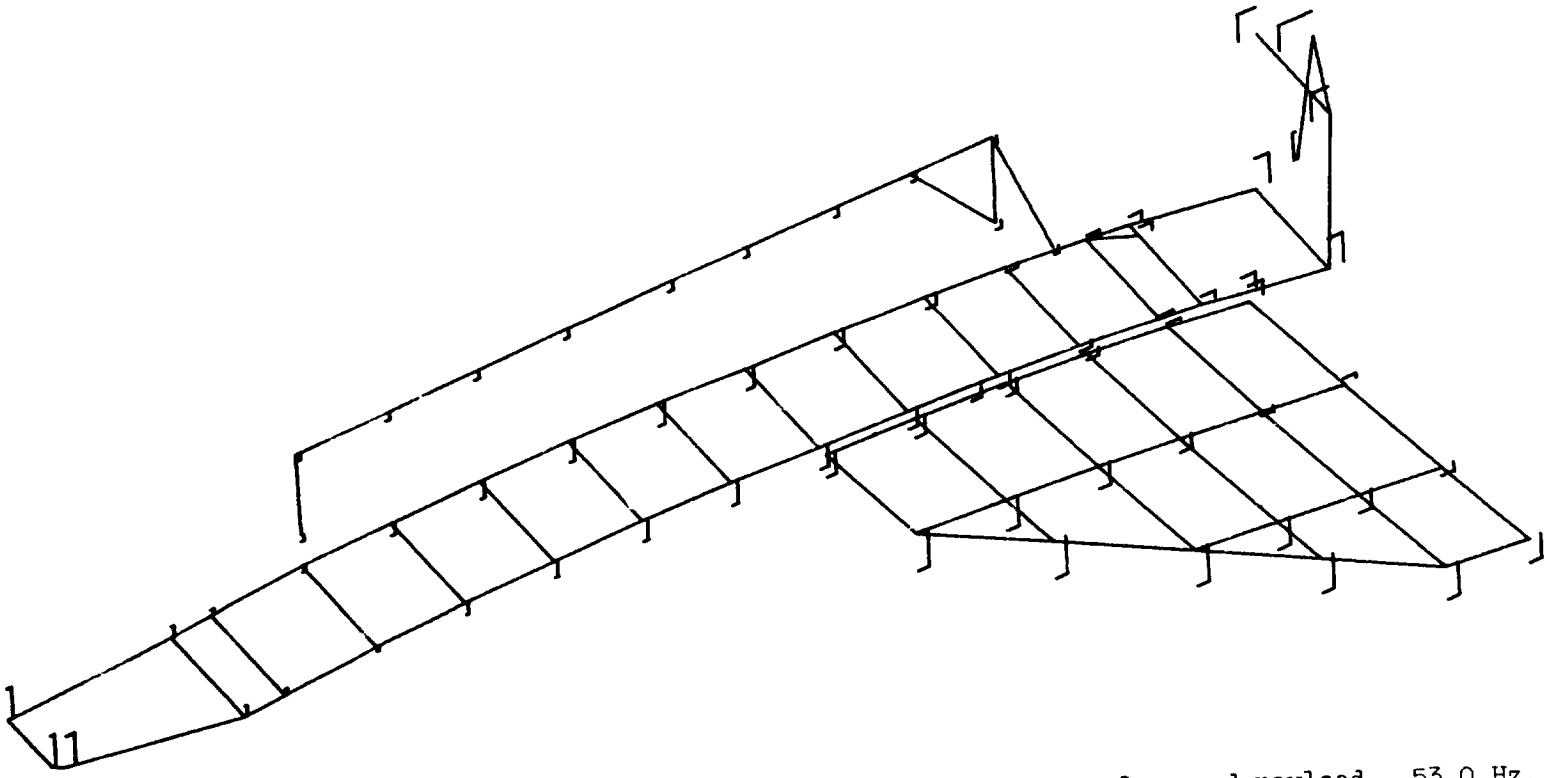

Figure 24.- First elastic symmetric mode of orbiter showing bottom surface and payload. 53.0 Hz.

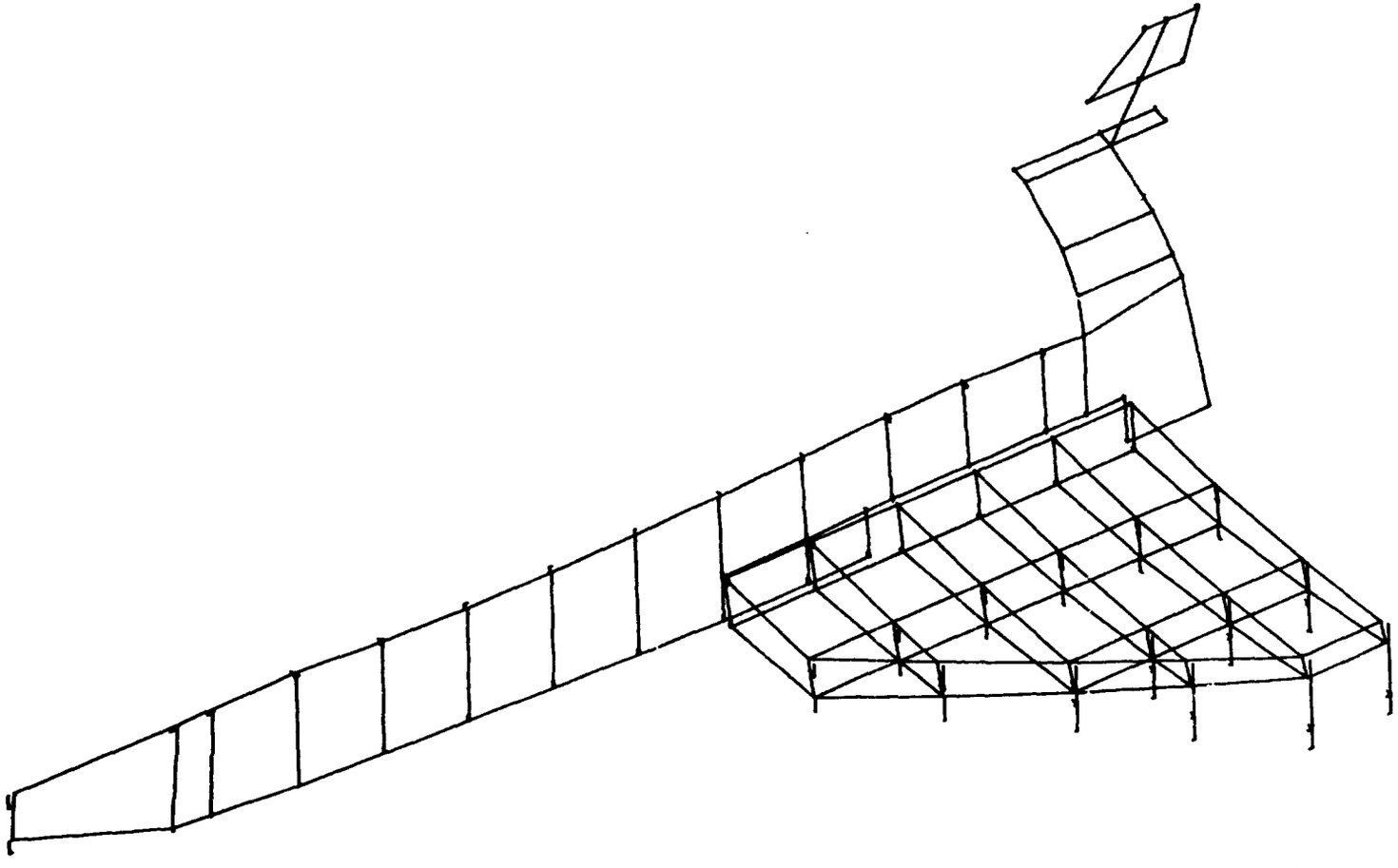

Figure 25.- Second elastic symmetric mode of orbiter showing fuselage and wing. 62.6 Hz.

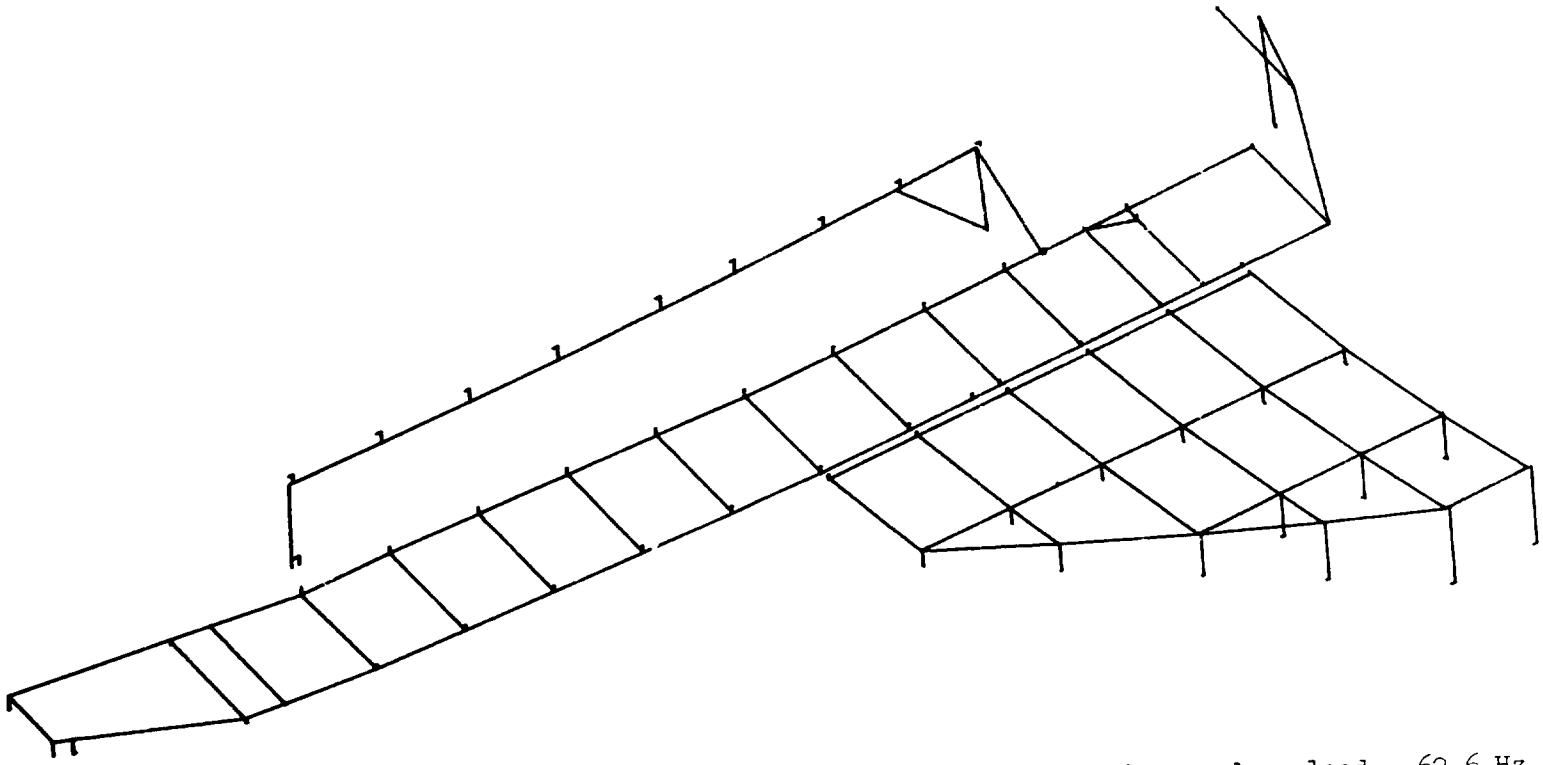

Figure 26.- Second elastic symmetric mode of orbiter showing bottom surface and payload. 62.6 Hz.

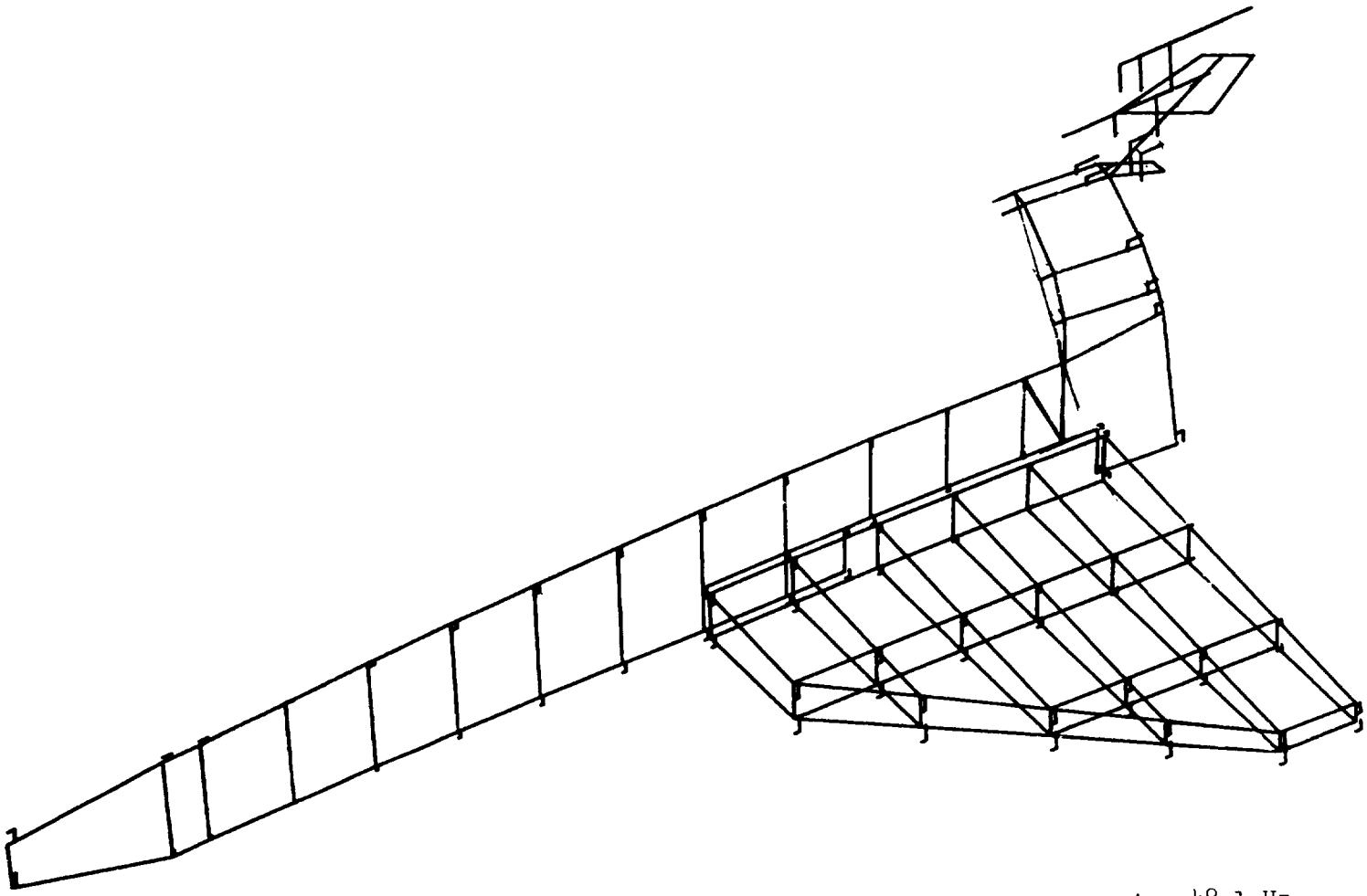

Figure 27.- First elastic symmetric mode of orbiter with forward fin spar cut. 48.1 Hz.

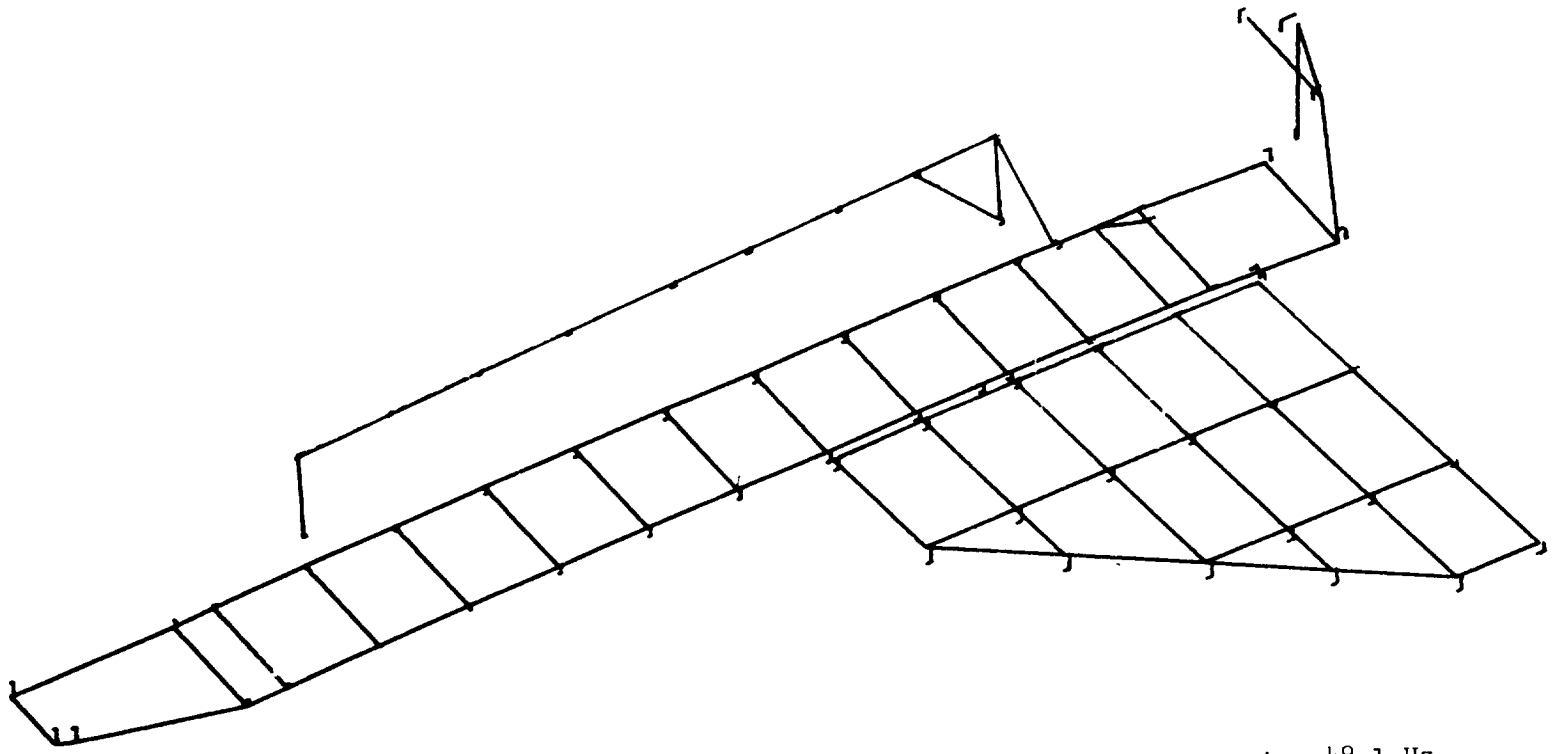

Figure 28.- First elastic symmetric mode of orbiter with forward fin spar cut. 48.1 Hz.

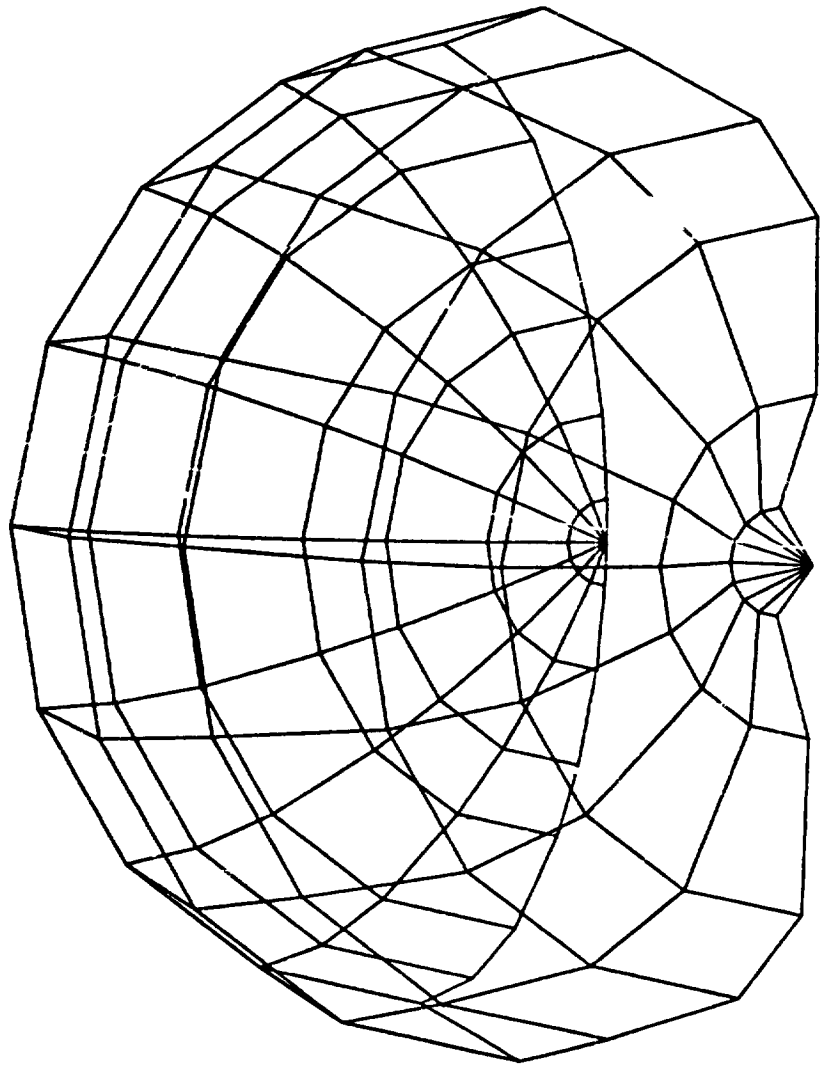

Figure 29.- Deformation of tank dome under 6.9 kN/m^2 (1 psi) showing original and deformed shapes.

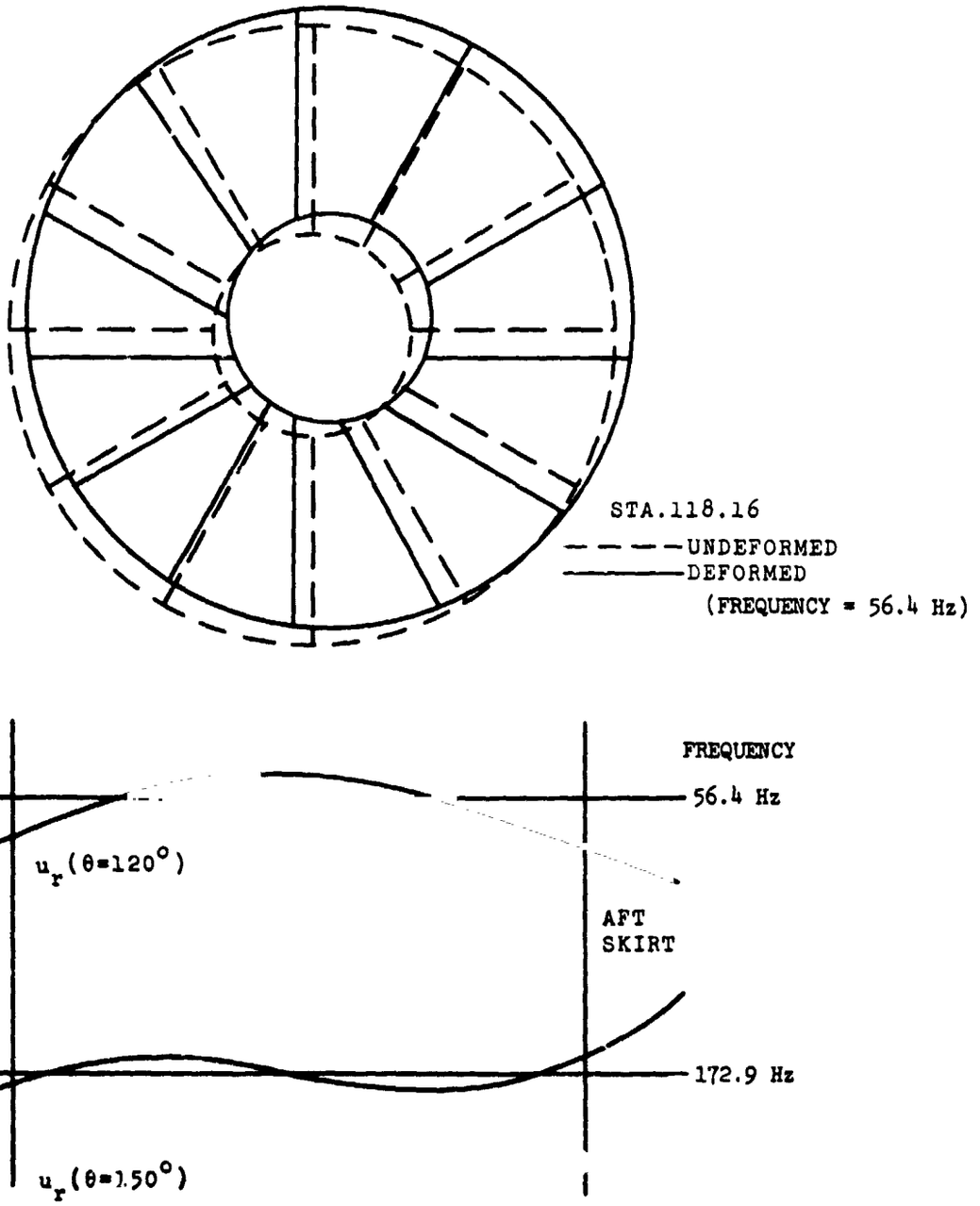

(a) First and second free bending modes.

Figure 30.- Shape for SRB modes.

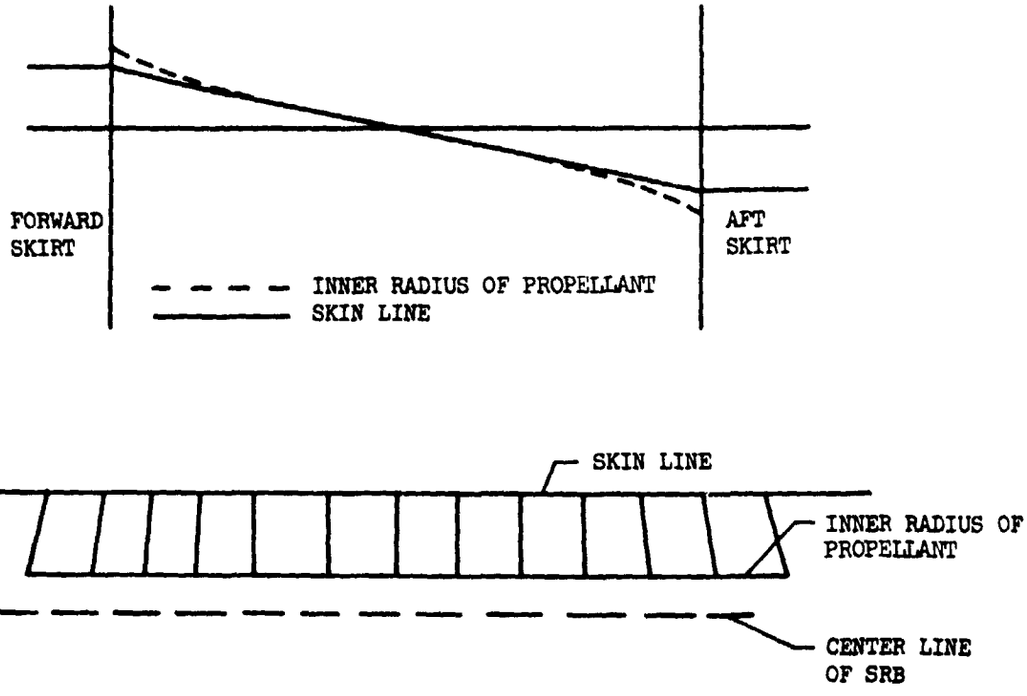

(b) Free longitudinal rod mode showing longitudinal thickness shear deflection. 196.0 Hz.

Figure 30.- Concluded.

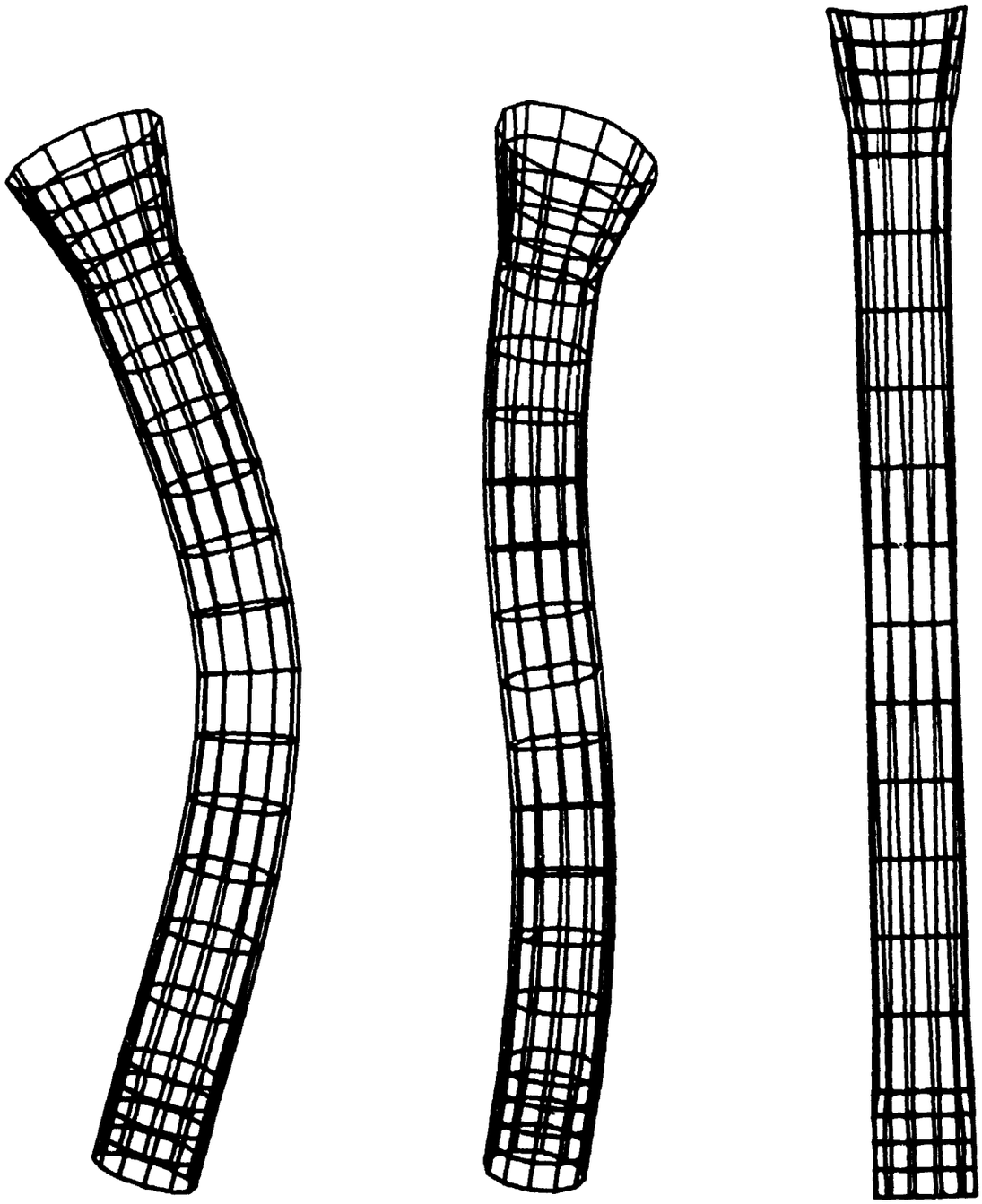

(a) First free bending mode. 56.4 Hz.

(b) Second free bending mode. 173.0 Hz.

(c) Longitudinal mode showing some torsion. 196.1 Hz.

Figure 31.- Shapes for SRB bending modes.